

# Indole Inhibitors of MMP-13 for Arthritic Disorders

Steven J. Taylor,\* Asitha Abeywardane, Shuang Liang, Zhaoming Xiong, John R. Proudfoot, Bennett Sandy Farmer, Donghong A. Gao, Alexander Heim-Riether, Lana Louise Smith-Keenan, Ingo Muegge, Yang Yu, Qiang Zhang, Donald Souza, Mark Panzenbeck, Daniel Goldberg, Melissa Hill-Drzewi, Mariana Margarit, Brandon Collins, John Xiang Li, Ljiljana Zuvela-Jelaska, Jun Li, and Neil A. Farrow



Cite This: *ACS Omega* 2021, 6, 18635–18650

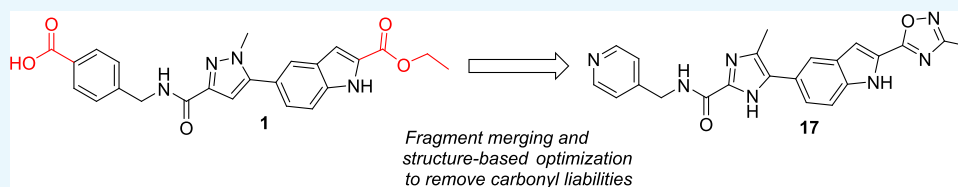


Read Online

ACCESS |

Metrics & More

Article Recommendations



**ABSTRACT:** Here, we described the design, by fragment merging and multiparameter optimization, of selective MMP-13 inhibitors that display an appropriate balance of potency and physicochemical properties to qualify as tool compounds suitable for *in vivo* testing. Optimization of potency was guided by structure-based insights, specifically to replace an ester moiety and introduce polar directional hydrogen bonding interactions in the core of the molecule. By introducing polar enthalpic interactions in this series of inhibitors, the overall beneficial physicochemical properties were maintained. These physicochemical properties translated to excellent drug-like properties beyond potency. In a murine model of rheumatoid arthritis, treatment of mice with selective inhibitors of MMP-13 resulted in a statistically significant reduction in the mean arthritic score vs control when dosed over a 14 day period.

## INTRODUCTION

Arthritis is broadly defined as inflammation in one or more joints, causing pain, stiffness, and debilitation that progress with age.<sup>1</sup> Arthritis can be further subdivided based upon disease etiology as osteoarthritis (OA, degenerative joint disease) and rheumatoid arthritis (RA, long-term autoimmune disorder).<sup>2</sup> Rheumatoid arthritis impacts over 1 million Americans, nearly 1% of the broader global population, and is three times more likely to occur in females. In addition to the quality of life burdens associated with reduced mobility and pain, patients with RA typically have lifespans 10–15 years shorter than their peers.<sup>3</sup> With an ever-aging global population coupled with the increase in autoimmune disorders, the need for improved pharmacological intervention to slow or reverse the debilitating impact of arthritis is apparent.

Pharmacological intervention for RA typically progresses from general anti-inflammatory agents such as nonsteroidal anti-inflammatory drugs and oral steroids to biologicals targeting TNF- $\alpha$  and IL6. More recently, several new oral therapies, JAK inhibitors,<sup>4</sup> have been approved for mild to moderate RA. We and others have looked to complement existing anti-cytokine-based therapies with therapies that directly prevent structural damage to the arthritic joints. Modulation of disease-driving enzymes expressed in the inflamed synovium and responsible for the degradation of articular collagen and other structural components of the joints represents an exciting approach to

disease treatment.<sup>5</sup> Inhibition of one such target class, metalloproteases,<sup>6</sup> presents an opportunity to prevent the structural damage associated with arthritis.

Matrix metalloproteases are calcium- and zinc-dependent enzymes that degrade several extracellular matrix proteins and bioactive molecules responsible for disease progression. Clinical use of nonselective metalloprotease inhibitors resulted in adverse events leading to the discontinuation and termination of development.<sup>7</sup> Specifically, musculoskeletal syndrome (MSS) that is associated with stiffening of the joints and musculature limited the development of pan-MMP inhibitors for oncology indications.<sup>8</sup> However, the absence of this joint inflammation and stiffness in the MMP-13 knockout mouse as well as human genetic variants suggested that selective inhibition of MMP-13 might be therapeutically beneficial and devoid of these side effects.<sup>9</sup> MMP-13 KO mice are protected from collagen antibody-induced arthritis, indicating that MMP-13 selective inhibition may have a therapeutic value for RA.<sup>10</sup> MMP-13

Received: March 11, 2021

Accepted: June 30, 2021

Published: July 19, 2021



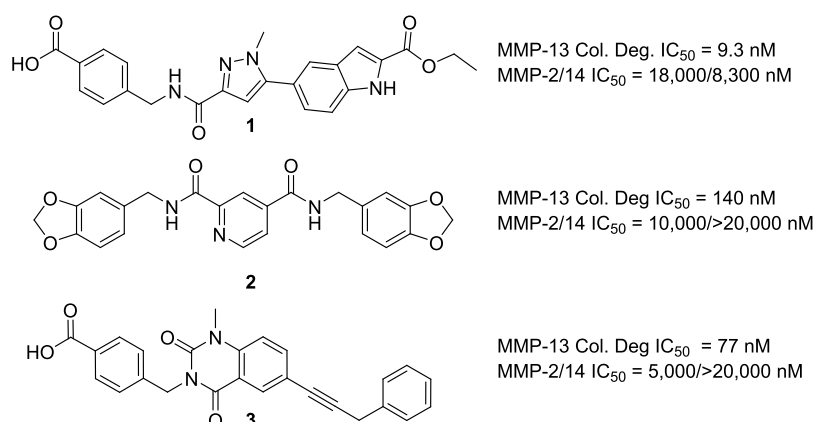


**Figure 1.** Reported MMP inhibitors that occupy the MMP-13 S1'\* selectivity pocket and their in vitro enzyme inhibition potencies.

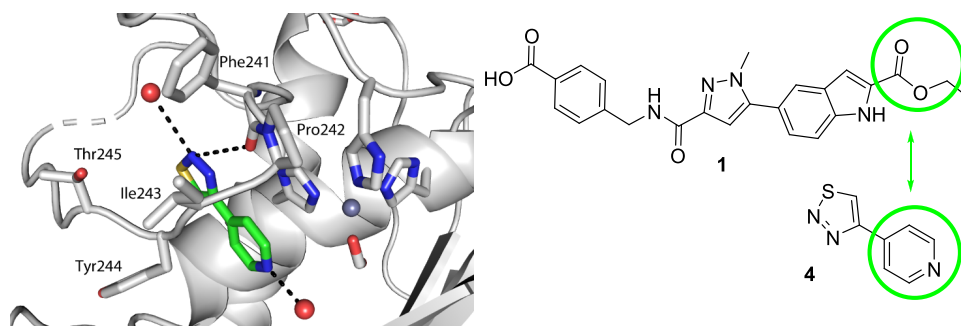


**Figure 2.** Cocrystal structure of **4** in MMP. The compound is positioned proximal to the triad of histidines, shown at right, that coordinate the catalytic zinc (pale blue sphere). Compound **4** makes two hydrogen bonds with bound waters (red spheres) and a hydrogen bond with the backbone carbonyl of Phe241. Compound **4** is completely enclosed within the protein. The scheme at right indicates the overlapping portions of **1** and **4**.

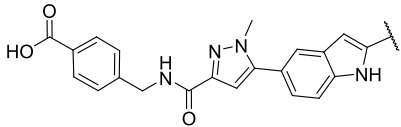
inhibition is beneficial in in vitro and in vivo models of arthritis, prompting several drug discovery campaigns aimed at developing selective MMP-13 inhibitors devoid of activity against other matrix-modifying proteins.

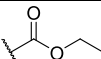
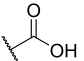
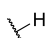
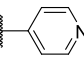
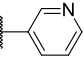
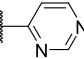
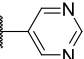
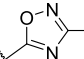
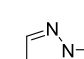
The first highly selective compounds were disclosed by teams at Aventis and Pfizer (**2**, Figure 1). Cocrystal structures of representative inhibitors with the catalytic subunit of MMP-13 revealed the origin of the observed selectivity. The high selectivity is attributed to the absence of direct interaction with the active site zinc, coupled with the occupancy of a deep pocket, the S1'\* pocket, that is inducible upon ligand binding and is significantly larger in MMP-13 than in other MMP isoforms.<sup>11</sup> In the apo form or crystal structures with fragments, this pocket is occluded by Thr245, which serves as a pseudo-gatekeeper preventing access. In fully elaborated inhibitors such as **1–3** (Figure 1), the sidechain of Thr245 is rotated, allowing the compounds to access this S1'\* selectivity pocket.

In compounds such as **1** and **3**, an additional key potency activity anchor is a direct salt bridge between Lys140 and the carboxylate group. Although beneficial for physicochemical properties and binding affinity, the carboxylate presents potential liabilities such as unstable acyl glucuronide formation and off-target activity against organic anion transporters.<sup>12</sup> As such, we focused on identifying alternatives for the carboxylate group in our second-generation inhibitors to attenuate risk in moving compounds forward into advanced profiling. In addition to highly potent and exquisitely selective MMP-13 inhibitors devoid of an acidic motif, we also required compounds to demonstrate the potential to robustly engage the target in vivo to maximize the opportunity of observing a pharmacological effect while determining if side effects of MMS could be decoupled

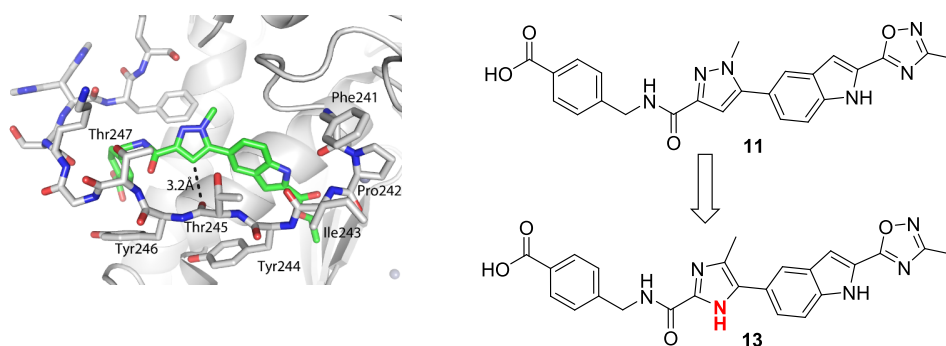
from the primary pharmacology. In the absence of robust PK/PD experiments, we set a target drug free fraction at  $C_{min}$  of  $>IC_{75}$  in the most relevant in vitro assay.<sup>13</sup> This preliminary exposure–efficacy relationship was selected based upon the high trough coverage typically needed to achieve efficacy by other known protease inhibitors.<sup>14</sup>

As described in previous reports,<sup>15,16</sup> our strategy to design extremely potent, selective inhibitors with excellent drug-like properties was grounded in a fragment-based approach and ligand efficiency-directed optimization. Initial efforts identified compound **1** that, although potent and selective, failed to achieve the free drug concentration at  $C_{min}$  relative to the potency required to robustly assess the drug concept in vivo. This was mainly due to high metabolic clearance leading to a modest/short half-life. The design of compounds that displayed a minimal shift in potency in the presence of added HSA, while improving clearance and being devoid of an acid motif, became a priority. Since the high clearance of **1** was due to ester hydrolysis, we focused on identifying a suitable metabolically stable ester replacement. Fragments are versatile as starting points for an optimization campaign but have also been successfully leveraged to “replace” liability-stricken motifs in more elaborated molecules.<sup>17</sup> In the course of our fragment screening campaign, biophysical and high concentration biochemical screening had identified pyridine thiadiazole **4** as a micromolar inhibitor of MMP-13 (Figure 2). Cocrystallization of **4** with MMP-13 revealed that the pyridyl motif occupied a similar region as the ester motif in **1**, with the same absence of any direct interaction with the zinc metal ion of MMP-13 (PDB code: 7JU8).<sup>18</sup> Based upon this observation as well as precedented ester bioisosteres, we focused the SAR on heteroaryl motifs as ester replacements.

Table 1. Ester Replacements Guided by Fragment 4<sup>a</sup>


Cpd.	Structure	MMP13 IC <sub>50</sub> MMP13 IC <sub>50</sub> (HSA)	mMMP13 IC <sub>50</sub>	MMP2/14 IC <sub>50</sub>	hLM (%Qh)	Sol. pH 4.5/7.4
1		0.8 4.1	18	18000/8300	40	0.1/64
5		2600 5600	NT	>24000/>24000	<11	0.3/47
6		>26000 NA	NT	>26000/>26000	25	0.1/>90
7		0.92 2.7	28	>22000/>20000	50	0.1/0.9
8		5.8 18	123	>20000/>20000	<11	3/15
9		0.81 2.9	50	>20000/NA	20	0.1/21
10		6.8 31	176	>20000/>20000	76	0.2/45
11		0.21 1.2	NT	>20000/>20000	<11	0.4/45
12		1.6 8.2	3.5	>20000/>20000	62	0.2/40

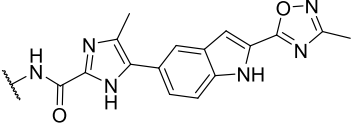
<sup>a</sup>In vitro enzyme IC<sub>50</sub> values are represented as nM and averaged from a minimum of two independent determinations; HSA, 1.25% human serum albumin added to the biochemical assay to gauge potential for protein shift in vivo. Human liver microsome (hLM) values are represented as a percent of liver blood flow. Kinetic solubility (Sol) solubility in  $\mu\text{g/mL}$ .

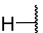
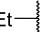
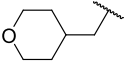
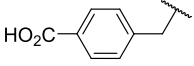
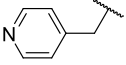
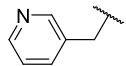
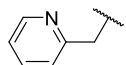
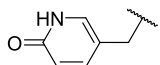
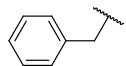


**Figure 3.** Structural insight suggests imidazole as a more optimal replacement for the pyrazole moiety. The crystal structure of a related compound from a previous study (PBD code: SBPA) reveals that the 3-carbon of the pyrazole ring is 3.2 Å from the backbone carbonyl oxygen of Thr245.

The initial SAR of ester surrogates is shown in Table 1. The importance of the ester motif is highlighted by the observation that carboxylic acid **5** or truncated analog **6** is inactive in the MMP-13 biochemical assay. These modifications, however, increased the overall metabolic stability of the compounds, highlighting the opportunity to optimize both stability and potency with modifications in this region of the molecule. Replacement of the ester with the 4-pyridine motif present in fragment **4** gave **7**, which was equipotent to ester **1** (Table 1).

The directionality of the pyridine hydrogen bond acceptor was critical in maintaining potency, as the 3-pyridyl (**8**) or 3,5-pyrimidine (**10**) analogs were significantly less active than **7**, while the 2,4-pyrimidine **9** maintained comparable potency to pyridine analog **7**. Given these observations, five-member heteroaryls with hydrogen bond acceptors at the 3 or 5 position were also investigated to optimize the trajectory of the HBA motifs. Pyrazole **12** and oxadiazole **11** both maintained acceptable potency compared to ester **1** and had a modest

Table 2. Acid Replacement Motifs on Fully Elaborated Imidazole Inhibitors<sup>a</sup>


Cpd.	Structure	MMP13 IC <sub>50</sub> MMP13 IC <sub>50</sub> (HSA)	mMMP13 IC <sub>50</sub>	MMP2/14 IC <sub>50</sub>
14		16 37	67	>20000/>28000
15		11 34	30	>20000/>20000
16		1.1 4.8	60	>20000/>20000
13		0.27 1.4	0.4	>20000/>20000
17		0.45 1.3	4	>20000/>20000
18		0.64 1.7	9	>20000/>20000
19		3.1 10	19	>20000/>20000
20		0.33 1.0	3	>24000/>24000
21		2.3 8.8	34	>20000/>20000

<sup>a</sup>In vitro enzyme IC<sub>50</sub> values are represented as nM and averaged from a minimum of two independent determinations; HSA, 1.25% human serum albumin added to the biochemical assay to gauge potential for protein shift in vivo.

shift in the presence of serum proteins, also in line with the impact of HSA for the activity of **1**. Additionally, oxadiazole **11** displayed an acceptable in vitro clearance as measured by human liver microsomes (<11% Qh). All compounds showed a >5-fold activity shift in the presence of human serum, however, suggesting that the class would have high protein binding and low free fraction in vivo. All compounds in addition to **1** showed 10–30-fold weaker potency against the murine MMP-13 enzyme, indicating an additional potency/PK burden in robustly challenging the drug concept in murine models in vivo.<sup>19</sup> Finally, compounds had low aqueous solubility at pH 4.5 and high solubility at neutral pH as expected for carboxylates.

To overcome the expected series-wide low free fraction in vivo, we sought to incorporate additional enthalpic-driven activity anchors into the scaffold.<sup>20</sup> Enthalpic interactions are typically polar and should decrease lipophilicity, which is inversely correlated to the available free drug. The crystal structure of **1** (PDB code: 5BPA) showed that the backbone carbonyl of Thr245 lie within 3.2 Å of C-4 of the pyrazole core and in a geometry consistent with the introduction of a direct interaction with a hydrogen bond donor (Figure 3). Modification of the pyrazole ring to an imidazole would allow a favorable hydrogen bond interaction while decreasing log*P* and in turn improving free drug concentration. Guided by this

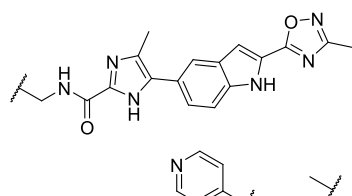
insight, we generated imidazole **13**, which maintained potent intrinsic activity with improved activity in the presence of serum protein, indicative of a higher free drug concentration than the corresponding pyrazole analog.

With the ester liability addressed and the intrinsic activity and free fraction improved by the core modifications, we sought to replace the terminal carboxylic acid, which carries potential DDI and metabolic liabilities. A focused library was designed to systematically explore the S1'\* pocket with the goal of removing the acid moiety while maintaining or improving potency (Table 2). The terminal acidic group in **1** makes a hydrogen bonding interaction with the partially solvent-exposed Lys140. This interaction is a critical contributor to the inhibition of MMP-13, since the unsubstituted phenyl analog, **21**, is 10-fold less potent than **13**. Removal of the benzoate group entirely, as in **14**, resulted in an order magnitude loss in intrinsic activity. Insertion of a small aliphatic linker did not regain the activity lost by removing the terminal ring system (Table 2, **15**). Potency was recovered with aliphatic or aromatic methylene spaced ring systems (Table 2, entries 3–9). The potency of the inhibitors could be maintained with a variety of aryl motifs, and metabolic clearance could be attenuated by adjusting the overall clog*P* of the compounds (Table 2, entries 5–8). Except for the 2-pyridyl isomer, all pyridine analogs were equipotent to inhibitor **1**. The

hydrogen bond acceptor from pyridines **17** and **19** could be externalized as well as shown by pyridone **20**, highlighting some level of flexibility for additional analoging in this region of the scaffold.

With suitable ester and carboxylic acid replacements identified, we assessed the pharmacokinetic profile of selected inhibitors, **15** and **17**, to determine suitability as tool molecules. Compounds **15** and **17**, dosed in triplicate in rats, showed a moderate to low volume of distributions and moderate clearance with overall modest half-lives of 1.8 and 0.9 h, respectively (Table 3). The compounds were well absorbed (%F = 37 and 43, respectively) and achieved peak concentrations in the low micromolar range after standard suspension dosing at 3 mg/kg.

**Table 3.** Rat Pharmacokinetic Profile of **17** and **15**



Compound	<b>17</b>	<b>15</b>
iv AUC (nM <sup>h</sup> )	3000	2,400
VSS (L/kg)	1.5	1.3
CL (% Qh)	24	27
T <sub>1/2</sub> (h)	1.8	0.9
C <sub>max</sub> (nM)	2,200	2,600
po AUC (nM <sup>h</sup> )	11,100	10,300
%F	37	43

Given the acceptable in vitro pharmacokinetic profiles (Table 3), compounds **1** and **17** as well as the two literature comparator compounds **2** and **3** were further profiled in multiple in vitro functional assays along with cell permeability and protein binding assays to assess the potential of these compounds for in vivo studies. (Table 4). The four compounds spanned a two-logarithmic range in potency (1 nM to 141 nM) in an MMP-13-dependent collagen degradation functional assay. Surprisingly, compound **2** had a significant shift (>100×) in the collagen degradation vs the isolated MMP-13 enzyme that was not observed with the other chemical classes (data not shown). All four compounds demonstrated acceptable permeability predicted in active and passive in vitro assays (Caco-2 and

PAMPA). They also demonstrated potent inhibition of native collagen degradation in the cartilage explant assay in vitro (BNC degradation, Table 4). In addition, all compounds were extremely selective against all the other MMP isoforms tested (Table 4), as expected based upon the structural data and the design to fully occupy the MMP-13 S1'\* selectivity pocket.

Compounds **1**, **17**, **2**, and **3** were dosed in female B10.RIII mice, the species and strain used for the murine mechanistic models, to determine if the pharmacokinetic profiles were suitable to engage the target (Figure 4). It was important to

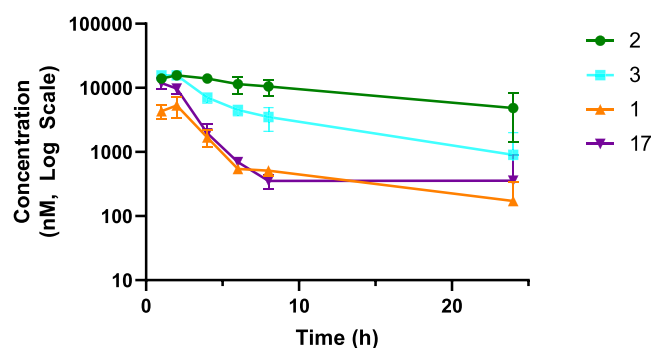


**Figure 4.** Plasma exposure of MMP-13 inhibitors in mice upon oral dosing @100 mpk.

ensure that free drug exposures at C<sub>min</sub> adequately covered the potency of the compounds in the murine MMP13 assay. All four compounds reached micromolar exposure levels after suspension PK dosing, and exposures over 100 nM were maintained through 8 h. Given the high potency in the collagen degradation assay in vitro (Table 4), as well as the acceptable free fraction, compounds **1**, **2**, **3**, and **17** were advanced into murine collagen antibody-induced arthritis (CAIA) studies (Figure 5).<sup>21</sup> Briefly, an anti-collagen type II monoclonal antibody cocktail was administered via intraperitoneal injection, followed 3 days later by intraperitoneal injection with LPS to initiate disease. Beginning on day 4, mice were dosed twice daily by oral gavage with compounds (100 mg/kg) or vehicle control. The mean arthritic score for each dosing group was measured daily, and body weight was measured on every other day. Over 14 days of treatment, none of the treatment groups showed statistically significant body weight changes vs control groups, indicating that the compounds were well tolerated. At the end of the study (day 14), inhibitors **1**, **3**, and **17** significantly reduced the overall mean arthritic score vs vehicle control. Compound **2**, with lower potency as well as a lower free fraction, did not reduce the mean arthritic score vs control animals.

**Table 4.** Extended Profiling of Compound Candidates for Potential In Vivo Study

	compound 1	compound 17	compound 2	compound 3
MMP-13 collagen Degradation assay (IC <sub>50</sub> , nM)	9.3	1.2	77	140
BNC degradation assay (IC <sub>50</sub> , nM)	43	25	350	87
Caco-2 (AB/BA) (×10 <sup>-6</sup> cm/s)	0.6/15	3.5/9	NT	NT
PAMPA (cm/s)	3.3 × 10 <sup>-6</sup>	2.9 × 10 <sup>-5</sup>	3 × 10 <sup>-7</sup>	7.1 × 10 <sup>-5</sup>
hPPB (% bound)	91	93	98	99
MMP (IC <sub>50</sub> , μM): 1, 2, 3, 7, 8, 9, 10, 12, 14	0.72, 18, >20, >20, >20, >20, >20, >20, 8.3	>20, 20, >20, >20, 3.1, >20, >20, 10, >20	>20, >20, >20, >20, >20, >20, >20, >20, >20	>20, 10, >20, >20, >20, >20, >20, 10, >20

<sup>a</sup>In vitro collagen degradation and cartilage degradation IC<sub>50</sub> values are represented as nM and averaged from a minimum of two independent determinations; BNC, bovine nasal cartilage.

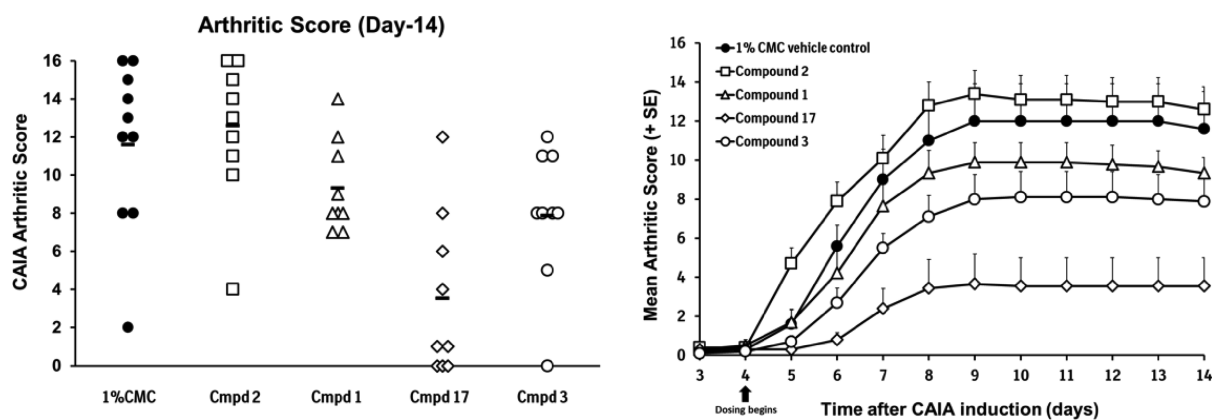
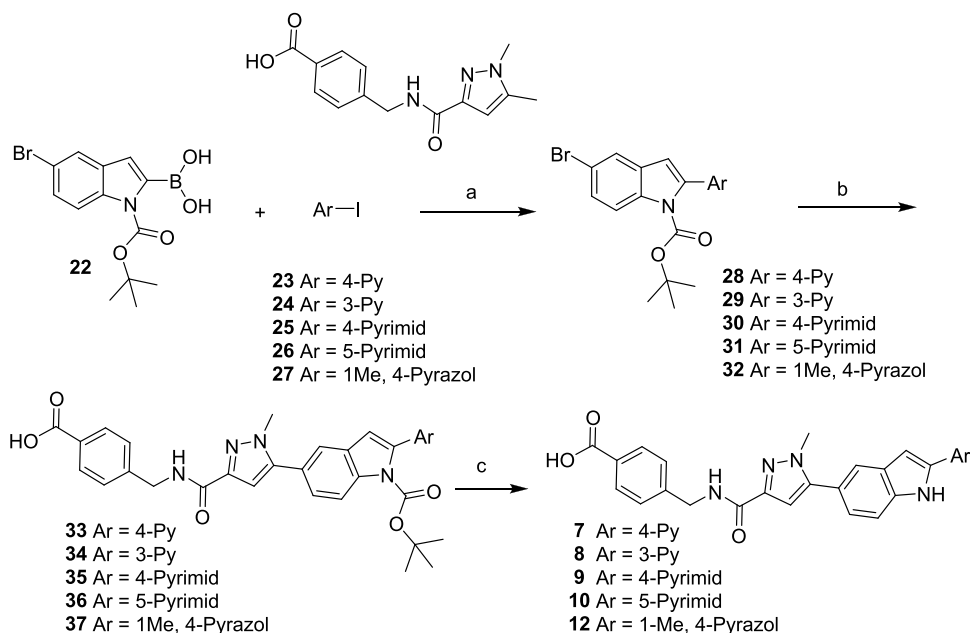


**Figure 5.** In vivo efficacy of compounds 1, 2, 3, and 17 in murine collagen antibody-induced arthritis. Significance testing was conducted on the groups' scores at day 14 using the Mann–Whitney  $U$  test with  $p = 0.05$ . Compound treatment group scores were tested to the vehicle control group scores with  $p < 0.05$  being considered statistically significant. Compound 2,  $p = 0.667$ ; compound 1,  $p = 0.025$ ; compound 17,  $p = 0.001$ ; compound 3,  $p = 0.03$ .

### Scheme 1. Synthesis of Compounds 7–10 and 12<sup>a</sup>



<sup>a</sup>Reagents and conditions: (a) Pd(dppf)Cl<sub>2</sub>, 1,4-dioxane/water, Cs<sub>2</sub>CO<sub>3</sub>; (b) bis(pinacolato)diboron, Pd(dppf)Cl<sub>2</sub>, 1,4-dioxane, KOAc, 4-((5-bromo-1-methyl-1H-pyrazole-3-carboxamido)methyl)benzoic acid, Pd(dppf)Cl<sub>2</sub>, 2 M aq. Na<sub>2</sub>CO<sub>3</sub>, DMF; (c) TFA, CH<sub>2</sub>Cl<sub>2</sub>.

## CONCLUSIONS

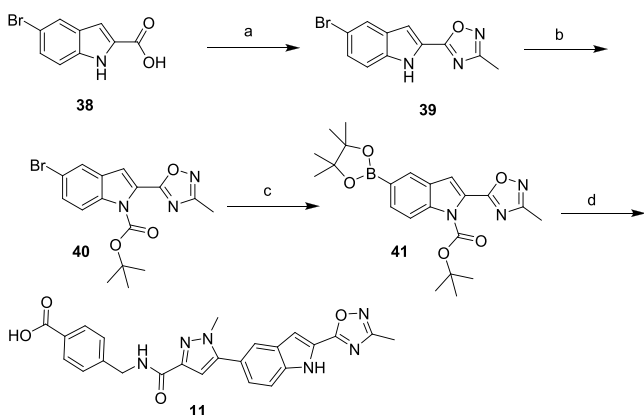
We have shown that neither the ester nor the carboxylic acid functional groups previously disclosed as critical binding motifs in highly potent and selective MMP-13 inhibitors are essential, and both can be successfully replaced.<sup>22</sup> The strategy leveraged to achieve this relied on fragment “merging” as well as fragment and structure-based drug design.<sup>23</sup> By coupling medicinal chemistry with structural insights, optimization of ligands can take place in a more rational manner, allowing for selective introduction of potency anchors without compromising drug-like properties. A set of selective MMP-13 inhibitors with sufficient activity in a functionally relevant assay and with an acceptable pharmacokinetic profile allowed for testing the benefit of MMP-13 inhibition in an in vivo mechanistic model of disease. While extensive PK/PD efficacy relationships cannot be determined by these initial studies, compounds described within should serve as appropriate tool molecules to further elucidate the role of MMP-13 inhibition in the progression of disease.

## CHEMISTRY

Compounds 1, 5, and 6 were prepared as previously described. Pyridine thiazazole 4 was obtained from commercial sources. Literature inhibitors 2<sup>24</sup> and 3<sup>25</sup> were obtained utilizing the published procedures.

2-Arylindoles 7–10 and 12 were prepared as described in Scheme 1. Commercially available BOC-protected boronic acid 22 was selectively coupled with aryl iodides 23–27 under palladium-catalyzed Suzuki conditions to afford 6-bromo-2-aryl indoles 28–32. 6-Bromo-2-aryl indoles 28–32 were then coupled with 4-((5-bromo-1-methyl-1H-pyrazole-3-carboxamido)methyl)benzoic acid, followed by acid-mediated deprotection of the N-Boc protecting group to afford 2-aryl indole acids 7–10 and 12.

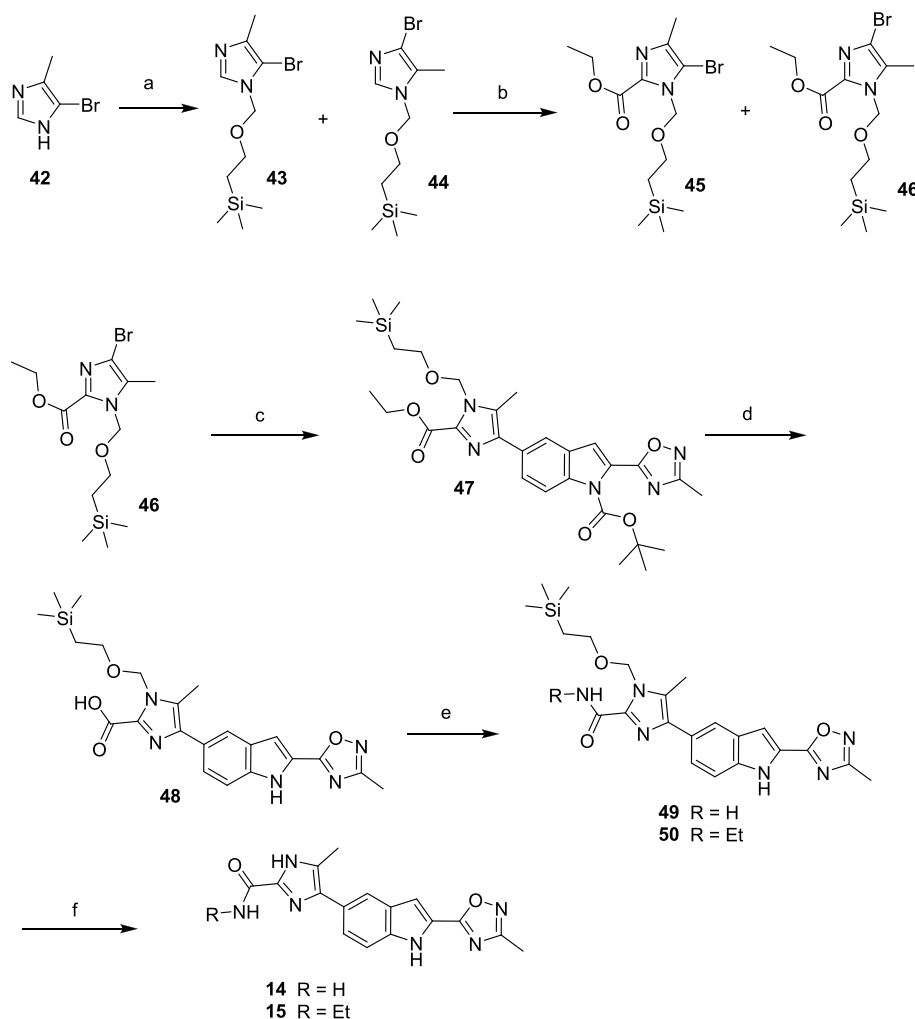
Oxadiazole 11 was prepared as outlined in Scheme 2. Commercially available indole acid 38 was treated with *N*-hydroxyacetamide under standard coupling conditions to afford 2-indole oxadiazole 39. The nitrogen in indole 39 was then

Scheme 2. Synthesis of Compound 11<sup>a</sup>

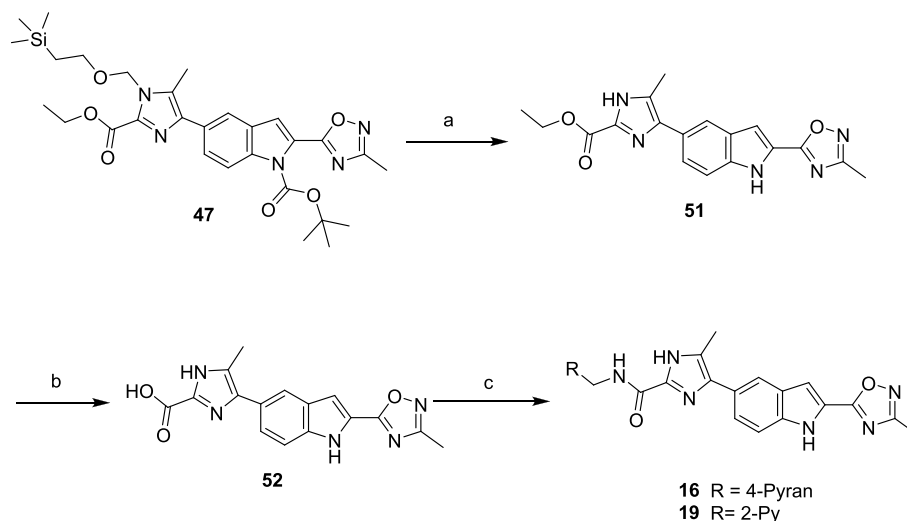
<sup>a</sup>Reagents and conditions: (a) *N*-hydroxy-acetamide, TEA, TBTU, DMF; (b) di-*tert*-butyl dicarbonate, DMAP, DMF; (c) bis(pinacolato)diboron, Pd(dppf)Cl<sub>2</sub>, 1,4-dioxane, K<sub>2</sub>CO<sub>3</sub>; (d) 4-((5-bromo-1-methyl-1H-pyrazole-3-carboxamido)methyl)benzoic acid, bis(di-*tert*-butyl(4-dimethylaminophenyl)phosphine)dichloropalladium(II), 2 M aq. Na<sub>2</sub>CO<sub>3</sub>, DMF.

BOC-protected to provide 40, which was then treated with bis(pinacolato)diboron and palladium to afford boronic ester 41. Boronic ester 41 was treated with 4-((5-bromo-1-methyl-1H-pyrazole-3-carboxamido)methyl)benzoic acid to yield the fully elaborated oxadiazole 11.

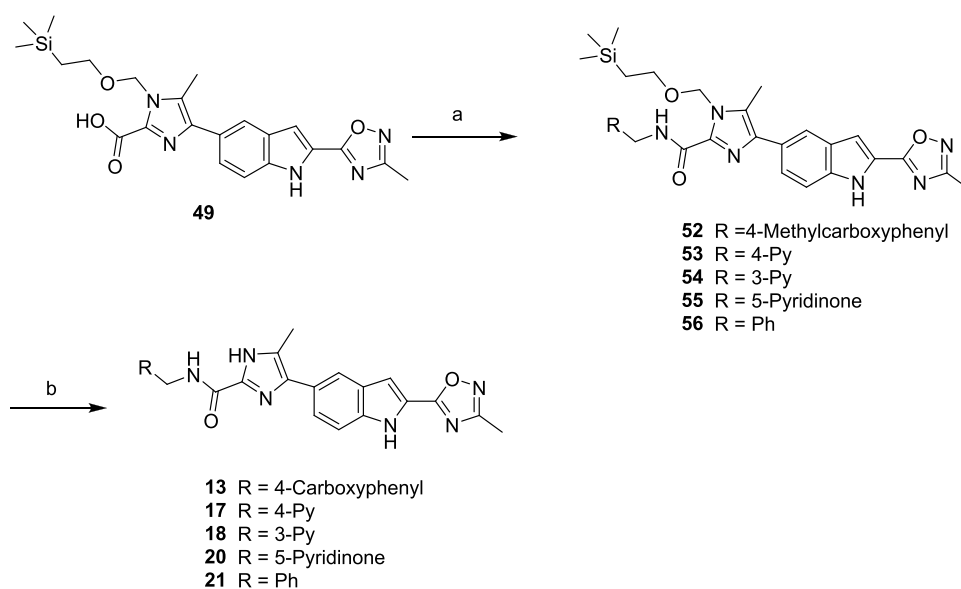
Oxindole analogs 14 and 15 were synthesized as outlined in Scheme 3. 5-Bromo-4-methyl imidazole was treated with SEM-Cl to afford a 1:1 mixture of SEM-protected imidazoles 43 and 44. Compounds 43 and 44 were treated at a low temperature with LDA, and the resulting anion was trapped with ethyl chloroformate to afford intermediate esters 45 and 46 that were separated by column chromatography. Regioisomer 46 was coupled with 41 under palladium-catalyzed conditions to afford the fully protected 7-imidazole indole 47. Ethyl ester 47 was treated with sodium hydroxide in a slurry of THF/water to afford acid 48. Acid 48 was purified by direct precipitation to afford the sodium salt and used directly or stored as a solid at -20 °C. Attempts to further purify intermediate 48, either as the sodium salt or as the free acid by normal or reversed-phase column chromatography, resulted in decarboxylation and further compound degradation. Sodium salt 48 was reacted under standard amide coupling conditions with either ethyl

Scheme 3. Synthesis of Compounds 14 and 15<sup>a</sup>

<sup>a</sup>Reagents and conditions: (a) NaH, THF, (2-chloromethoxy-ethyl)-trimethyl-silane; (b) LDA, THF, ethyl chloroformate; (c) 41, bis(di-*tert*-butyl(4-dimethylaminophenyl)phosphine)dichloropalladium(II), Na<sub>2</sub>CO<sub>3</sub>, toluene; (d) NaOH, THF/MeOH; (e) 1-ethyl-3-(3-dimethylaminopropyl)carbodiimide hydrochloride, HOBT, DMF, ammonium hydroxide for 57/ethyl amine for 58; (f) HCl, ethanol.

Scheme 4. Synthesis of Compounds 16 and 19<sup>a</sup>

<sup>a</sup>Reagents and conditions: (a) TFA, CH<sub>2</sub>Cl<sub>2</sub>; (b) LiOH, 1,4-dioxane/water; (c) (tetrahydro-2H-pyran-4-yl)methanamine (for **16**), pyridin-2-ylmethanamine (for **19**), HATU, HOAt, DIPEA, DMF.

Scheme 5. Synthesis of Compounds 13, 17, 18, 20, and 21<sup>a</sup>

<sup>a</sup>Reagents and conditions: (a) methyl 4-(aminomethyl)benzoate (**52**), pyridin-4-ylmethanamine (**53**), pyridin-3-ylmethanamine (**54**), 5-(aminomethyl)pyridin-2(1H)-one (**55**), benzylamine (**56**), HATU, HOAt, DIPEA, DMF; (b) HCl, 1,4-dioxane.

amine or ammonium hydroxide to afford amides **49** and **50**. Amides **49** and **50** were then treated with a strong acid to remove the SEM protecting groups, affording imidazoles **14** and **15**.

Amides **16** and **19** were prepared by initial bis-deprotection of imidazole **47** to give **51**, which was saponified to acid **52**, isolated as the lithium salt (Scheme 4). Like intermediate **48**, **52** was used directly in the next coupling sequence or stored at  $-20^{\circ}\text{C}$  due to a tendency to decarboxylate at room temperature. Intermediate **52** was treated with either 2-pyridylbenzylamine or 4-pyranyl methylamine under standard amide coupling conditions to afford analogs **16** and **19**.

Compounds **13**, **17**, **18**, **20**, and **21** were synthesized as shown in Scheme 5. Intermediate acid **48** was treated with commercially available benzylamines under standard amide

bond formation conditions to afford imidazole-protected amides **52–56**. Intermediates **52–56** were treated with a strong acid to afford imidazoles **13**, **17**, **18**, **20**, and **21**.

## CHEMISTRY GENERAL REMARKS

Starting materials were obtained from commercial suppliers and used without further purification, unless otherwise stated. The <sup>1</sup>H NMR spectra were recorded on a Bruker UltraShield-400 MHz spectrometer operating at 400 MHz in solvents, as noted. Proton coupling constants (*J* values) are rounded to the nearest Hz. All coupling constants are reported in hertz (Hz), and multiplicities are labeled s (singlet), bs, (broad singlet), d (doublet), t (triplet), q (quartet), dd (doublet of doublets), dt (doublet of triplets), and m (multiplet). All NMR spectra were referenced to tetramethylsilane (TMS). All solvents were of



HPLC grade or higher. The reactions were followed by TLC on precoated Uniplate silica gel plates purchased from Analtech. The developed plates were visualized using 254 nm UV illumination or by PMA stain. Flash column chromatography on silica gel was performed on Redi Sep prepacked disposable silica gel columns using an Isco Combiflash Biotage SP1 or on traditional gravity columns. Reactions were carried out under an argon atmosphere at room temperature, unless otherwise noted. All compounds were of >95% purity or higher as noted in the text. Mass spectroscopy data were obtained using the Micromass Platform LCZ (flow injection). In addition to mass spectrometry and NMR, purity was evaluated by:

- System 1: Analytical HPLC using a Varian Dynamax SD-200 pump coupled to a Varian Dynamax UV-1 detector: the solvents were as follows: (A) water + 0.05% TFA and (B) acetonitrile + 0.05% TFA; flow, 1.2 mL/min. Column Vydac RP-18, 5 m, 250 × 4.6 mm, photodiode array detector at 220 nm; from 95% to 20% solvent (A) over 25 min.
- System 2: HP 1110 Agilent LCMS using a Quaternary G1311A pump coupled to a Micromass Platform LCZ detector: the solvents were as follows: (A) water + 0.1% formic acid and (B) acetonitrile + 0.1% formic acid; flow, 1.5 mL/min. Photodiode array detector at 190 or 400 nm; (a) Agilent Zorbax Eclipse XDB-C8 5 μm, 4.6 × 150 mm column, 4.6 × 30 mm, 3.5 μm, from 99% to 5% solvent (A) over 10 min; or (b) Column Agilent Zorbax C18 SB 3.5 μm, 4.6 × 30 mm cartridge, from 95% to 5% solvent (A) over 2.5 min.

**4-([1-Methyl-5-(2-pyridin-4-yl-1H-indol-5-yl)-1H-pyrazole-3-carbonyl]-amino)-methyl-benzoic Acid (7).** 4-Iodopyridine (301 mg, 1.47 mmol), 5-bromo-1-(*tert*-butoxycarbonyl)-1H-indol-2-yl-boronic acid **22** (500 mg, 1.47 mmol), bis(di-*tert*-butyl(4-dimethylaminophenyl)phosphine)dichloropalladium(II) (72 mg, 0.088 mmol), and cesium carbonate (716 mg (2.2 mmol) were placed into a microwave vial and suspended in 1,4-dioxane/water (13 mL, 2 mL). The reaction vessel was sealed and heated in a microwave reactor for 20 min at 90 °C. The solution was diluted with EtOAc and filtered through a Celite pad. The pad was washed with DCM/methanol (1:1) and the combined extracts were washed with water and then brine. The organic layer was dried over anhydrous Na<sub>2</sub>SO<sub>4</sub>, filtered, and evaporated in vacuo. The crude product was purified on silica (EtOAc/hexane) to give 5-bromo-2-pyridin-4-yl-indole-1-carboxylic acid *tert*-butyl ester **28** (421 mg, 76%) as a pale white solid, which was used directly without further purification.

A flask was charged with 5-bromo-2-pyridin-4-yl-indole-1-carboxylic acid *tert*-butyl **28** (80 mg, 0.21 mmol), bis-(pinacolato)diboron (108 mg, 0.42 mmol), bis-diphenylferrocenylpalladium(II)dichloride (49 mg, 0.06 mmol), and potassium acetate (59 mg, 0.6 mmol), and the solids were suspended in 1,4-dioxane (2 mL). The reaction vessel was sealed and heated to 100 °C for 2 h under nitrogen and then cooled to room temperature. 4-[(5-Bromo-1-methyl-1H-pyrazole-3-carbonyl)-amino]-methyl-benzoic acid (72 mg, 0.21 mmol) and DMF (1 mL) were added under nitrogen, followed by 2 N aqueous Na<sub>2</sub>CO<sub>3</sub> solution (0.2 mL, 0.4 mmol) and bis-diphenylferrocenylpalladium(II)dichloride (20 mg). The reaction vessel was sealed and heated to 85 °C for 8 h. The solution was diluted with EtOAc and filtered through a Celite pad. The pad was washed with 15% ammonium hydroxide

(5 mL). The aqueous layer was separated and acidified by conc. HCl to pH 3, where a white solid precipitated from the solution. The solid was collected and the residual solvent was evaporated in vacuo to give 6-[5-(4-carboxy-benzylcarbamoyl)-2-methyl-2H-pyrazol-3-yl]-2-pyridin-4-yl-indole-1-carboxylic acid *tert*-butyl ester **33**, which was used directly without further purification.

To a solution of 6-[5-(4-carboxy-benzylcarbamoyl)-2-methyl-2H-pyrazol-3-yl]-2-pyridin-4-yl-indole-1-carboxylic acid *tert*-butyl ester (35 mg, 0.06 mmol) in dichloromethane (2 mL) was added TFA (2 mL). The mixture was stirred at room temperature for 30 min. The solvent was evaporated in vacuo and purified by reversed-phase HPLC to give the title compound **7** (20 mg, 69%). LCMS (ES+) *m/z* found, 452; retention time, 0.52 min. C<sub>26</sub>H<sub>21</sub>N<sub>5</sub>O<sub>3</sub> requires 452. HPLC: retention time, 7.88 min. <sup>1</sup>H NMR (400 MHz, DMSO-*d*<sub>6</sub>): ppm 12.85 (br, 1H), 12.33 (s, 1H), 8.84 (d, *J* = 6 Hz, 1H), 8.82 (d, *J* = 6.4 Hz, 2H), 8.25 (d, *J* = 6.4 Hz, 2H), 7.89 (d, *J* = 8.0 Hz, 2H), 7.85 (s, 1H), 7.61 (d, *J* = 8.4 Hz, 1H), 7.60 (s, 1H), 7.43 (d, *J* = 7.2 Hz, 1H), 7.41 (d, *J* = 8.4 Hz, 2H), 6.77 (s, 1H), 4.50 (d, *J* = 6.4 Hz, 2H), 3.93 (s, 3H).

**4-([1-Methyl-5-(2-pyridin-3-yl-1H-indol-5-yl)-1H-pyrazole-3-carbonyl]-amino)-methyl-benzoic Acid (8).** The title compound was prepared according to the procedure described for **7** from 5-bromo-1-(*tert*-butoxycarbonyl)-1H-indol-2-yl-boronic acid (250 mg, 0.73 mmol), 3-iodopyridine (150 mg, 0.73 mmol), bis(di-*tert*-butyl(4-dimethylaminophenyl)phosphine)dichloropalladium(II) (36 mg, 0.04 mmol), cesium carbonate (358 mg, 1.1 mmol), and 1,4-dioxane/water (13 mL/2 mL) to give 5-bromo-2-pyridin-3-yl-indole-1-carboxylic acid *tert*-butyl ester **29** (250 mg, 91%). 5-Bromo-2-pyridin-3-yl-indole-1-carboxylic acid *tert*-butyl ester **29** (100 mg, 0.26 mmol), bis(pinacolato)diboron (136 mg, 0.53 mmol), bis-diphenylferrocenylpalladium(II)dichloride (65 mg, 0.08 mmol), potassium acetate (78 mg, 0.80 mmol), 1,4-dioxane (2 mL), 4-[(5-bromo-1-methyl-1H-pyrazole-3-carbonyl)-amino]-methyl-benzoic acid (90 mg, 0.26 mmol), 2 N aqueous Na<sub>2</sub>CO<sub>3</sub> solution (0.3 mL, 0.6 mmol), and DMF (1 mL) were reacted to afford 6-[5-(4-carboxy-benzylcarbamoyl)-2-methyl-2H-pyrazol-3-yl]-2-pyridin-3-yl-indole-1-carboxylic acid *tert*-butyl ester **34** (25 mg, 17%). Deprotection of the BOC group gave the title product **8** (13 mg, 63%). LCMS (ES+) *m/z* found, 452; retention time, 0.2 min. C<sub>26</sub>H<sub>21</sub>N<sub>5</sub>O<sub>3</sub> requires 452. HPLC: retention time, 7.90 min. <sup>1</sup>H NMR (400 MHz, MeOH-*d*<sub>4</sub>): ppm 9.21 (s, 1H), 8.78 (dm, *J* = 8.4 Hz, 1H), 8.66 (d, *J* = 5.2 Hz, 1H), 7.98 (d, *J* = 8.4 Hz, 3H), 7.73 (s, 1H), 7.57 (d, *J* = 8.4 Hz, 1H), 7.45 (d, *J* = 8.4 Hz, 2H), 7.33 (dd, *J* = 8.4 Hz, 1.6 Hz, 1H), 7.24 (s, 1H), 6.80 (s, 1H), 4.64 (s, 2H), 3.93 (s, 3H).

**4-([1-Methyl-5-(2-pyrimidin-4-yl-1H-indol-5-yl)-1H-pyrazole-3-carbonyl]-amino)-methyl-benzoic Acid (9).** The title compound was prepared according to the procedure described for **7** from 5-bromo-1-(*tert*-butoxycarbonyl)-1H-indol-2-yl-boronic acid **22** (123 mg, 0.36 mmol), 4-iodopyrimidine (75 mg, 0.36 mmol), bis(di-*tert*-butyl(4-dimethylaminophenyl)phosphine)dichloropalladium(II) (29 mg, 0.04 mmol), cesium carbonate (177 mg, 0.54 mmol), and 1,4-dioxane/water (13 mL/2 mL) to give 5-bromo-2-pyrimidin-4-yl-indole-1-carboxylic acid *tert*-butyl ester **30** (71 mg, 52%). <sup>1</sup>H NMR (400 MHz, DMSO-*d*<sub>6</sub>): δ ppm 9.27 (d, *J* = 1.2 Hz, 1H), 8.91 (d, *J* = 5.2 Hz, 1H), 7.98 (d, *J* = 9.2 Hz, 1H), 7.95 (d, *J* = 2.0 Hz, 1H), 7.86 (dd, *J* = 5.2 Hz, 1.6 Hz, 1H), 7.57 (dd, *J* = 9.2 Hz, 2.0 Hz, 1H), 7.18 (s, 1H), 1.30 (s, 9H). 5-Bromo-2-pyrimidin-4-yl-indole-1-carboxylic acid *tert*-butyl ester **30** (71

mg, 0.19 mmol), bis(pinacolato)diboron (96 mg, 0.38 mmol), bis-diphenylferrocenylpalladium(II)dichloride (46 mg, 0.057 mmol), potassium acetate (55 mg, 0.57 mmol), 1,4-dioxane (2 mL), 4-[(5-bromo-1-methyl-1H-pyrazole-3-carbonyl)-amino]-methyl-benzoic acid (64 mg, 0.19 mmol), 2 N aqueous Na<sub>2</sub>CO<sub>3</sub> solution (0.2 mL, 0.4 mmol), and DMF (1 mL) were reacted to give 6-[5-(4-carboxy-benzylcarbamoyl)-2-methyl-2H-pyrazol-3-yl]-2-pyrimidin-4-yl-indole-1-carboxylic acid *tert*-butyl ester **35**, which was used for the next step without further purification. Deprotection of the BOC group with TFA yielded the title product **9** (13 mg, 19%). LCMS (ES+) *m/z* found, 453; retention time, 0.69 min. C<sub>25</sub>H<sub>20</sub>N<sub>6</sub>O<sub>3</sub> requires 453. HPLC: retention time, 9.03 min. <sup>1</sup>H NMR (400 MHz, DMSO-*d*<sub>6</sub>): ppm 12.88 (bs, 1H), 12.17 (s, 1H), 9.26 (d, *J* = 1.2 Hz, 1H), 8.87 (d, *J* = 5.6 Hz, 2H), 8.13 (dd, *J* = 5.6 Hz, 1.2 Hz, 1H), 7.94 (m, 2H), 7.87 (s, 1H), 7.65 (d, *J* = 7.6 Hz, 1H), 7.56 (d, *J* = 1.6 Hz, 1H), 7.46 (d, *J* = 8.0 Hz, 2H), 7.42 (dd, *J* = 8.4 Hz, 1.6 Hz, 1H), 6.80 (s, 1H), 4.54 (d, *J* = 6.0 Hz, 2H), 3.97 (s, 3H).

**4-[(1-Methyl-5-(2-pyrimidin-5-yl-1H-indol-5-yl)-1H-pyrazole-3-carbonyl)-amino]-methyl-benzoic Acid (10)**. The title compound was prepared according to the procedure described for **7** from 5-bromo-1-(*tert*-butoxycarbonyl)-1H-indol-2-yl-boronic acid **22** (500 mg, 1.47 mmol), 5-iodopyrimidine (233 mg, 1.47 mmol), bis(di-*tert*-butyl(4-dimethylaminophenyl)phosphine)dichloropalladium(II) (72 mg, 0.088 mmol), cesium carbonate (716 mg, 2.2 mmol), and 1,4-dioxane/water (13 mL/2 mL) to give 5-bromo-2-pyrimidin-5-yl-indole-1-carboxylic acid *tert*-butyl ester **31** (350 mg, 63%). 5-Bromo-2-pyrimidin-5-yl-indole-1-carboxylic acid *tert*-butyl ester **31** (69 mg, 0.18 mmol), bis(pinacolato)diboron (94 mg, 0.37 mmol), bis-diphenylferrocenylpalladium(II)dichloride (45 mg, 0.056 mmol), potassium acetate (54 mg, 0.58 mmol), 1,4-dioxane (2 mL), 4-[(5-bromo-1-methyl-1H-pyrazole-3-carbonyl)-amino]-methyl-benzoic acid (62 mg, 0.18 mmol), 2 N aqueous Na<sub>2</sub>CO<sub>3</sub> solution (0.2 mL, 0.4 mmol), and DMF (1 mL) were reacted to give 6-[5-(4-carboxy-benzylcarbamoyl)-2-methyl-2H-pyrazol-3-yl]-2-pyrimidin-5-yl-indole-1-carboxylic acid *tert*-butyl ester **36**, which was used for the next step without further purification. Deprotection of the BOC group with TFA yielded the title product **10** (22%). LCMS (ES+) *m/z* found, 453 min; retention time, 0.7 min. C<sub>25</sub>H<sub>20</sub>N<sub>6</sub>O<sub>3</sub> requires 453. HPLC: retention time, 8.9 min. <sup>1</sup>H NMR (400 MHz, DMSO-*d*<sub>6</sub>): ppm 12.84 (bs, 1H), 12.05 (s, 1H), 9.32 (s, 2H), 9.12 (s, 1H), 8.82 (t, *J* = 6.4 Hz, 1H), 7.89 (d, *J* = 8.4 Hz, 2H), 7.78 (s, 1H), 7.57 (d, *J* = 8.4 Hz, 1H), 7.41 (d, *J* = 8.0 Hz, 2H), 7.33 (dd, *J* = 8.4 Hz, 2.0 Hz, 1H), 7.27 (*J* = 1.6 Hz, 1H), 6.74 (s, 1H), 4.50 (d, *J* = 6.4 Hz, 2H), 3.92 (s, 3H).

**4-[(1-Methyl-5-[2-(3-methyl-[1,2,4]oxadiazol-5-yl)-1H-indol-5-yl]-1H-pyrazole-3-carbonyl)-amino]-methyl-benzoic Acid (11)**. A flask was charged with 5-bromo-1H-indole-2-carboxylic acid **38** (20 g, 83.3 mmol). The solid was dissolved in DMF (100 mL), and triethylamine (24 mL, 174.9 mmol) and TBTU (34.8 g, 91.6 mmol) were added. The reaction mixture was stirred at room temperature for 10 min. *N*-Hydroxyacetamide (6.7 g, 91.6 mmol) was added, and the mixture was stirred for 7 h at room temperature and then heated to 80 °C for 10 h. The mixture was cooled to room temperature and concentrated in vacuo. The resulting suspension was diluted with water. A solid was collected by filtration, washed three times with water, dried in vacuo to give 5-bromo-2-(3-methyl-[1,2,4]oxadiazol-5-yl)-1H-indole **39** (6.2 g, 22.2 mmol, 26%).

To a solution of 5-bromo-2-(3-methyl-[1,2,4]oxadiazol-5-yl)-1H-indole **39** (6.0 g, 21.5 mmol) and di-*tert*-butyl dicarbonate

(5.1 g, 23.7 mmol) in DMF (55 mL) was added DMAP (200 mg). The reaction was stirred at room temperature for 2 h. The solvent was removed in vacuo, and the residue was diluted with EtOAc and washed twice with water, then 10% citric acid solution, and brine. The organic layer was dried over anhydrous Na<sub>2</sub>SO<sub>4</sub>, filtered, and evaporated in vacuo, and the residue was purified over silica (EtOAc/heptane) to give 5-bromo-2-(3-methyl-[1,2,4]oxadiazol-5-yl)-indole-1-carboxylic acid *tert*-butyl ester **40** (8.0 g, 21.1 mmol, 98%), which was used without further purification. <sup>1</sup>H NMR (400 MHz, DMSO-*d*<sub>6</sub>): ppm 8.05 (d, *J* = 9.2 Hz, 1H), 8.00 (d, *J* = 2.0 Hz, 1H), 7.66 (dd, *J* = 9.2 Hz, 2.0 Hz, 1H), 7.43 (s, 1H), 2.46 (s, 3H), 1.42 (s, 9H).

A flask was charged with 5-bromo-2-(3-methyl-[1,2,4]oxadiazol-5-yl)-indole-1-carboxylic acid *tert*-butyl ester **40** (3.5 g, 9.2 mmol), potassium carbonate (3.1 g, 32.3 mmol), bis(pinacolato)diboron (3.5 g, 13.8 mmol), and bis-diphenylferrocenylpalladium(II)dichloride (2.2 g, 2.7 mmol) and dissolved in 1,4-dioxane (20 mL). The reaction was sealed and heated to 80 °C for 3 h, and then additional bis(pinacolato)diboron (3.5 g, 13.8 mmol) and bis-diphenylferrocenylpalladium(II)dichloride (2.2 g, 2.7 mmol) were added. The reaction was sealed and heated to 80 °C for another 3 h. The solution was cooled to room temperature and filtered through Celite and was washed with a copious amount of EtOAc. The combined organic layers were concentrated in vacuo and the resulting oil was purified by chromatography on silica gel (EtOAc/heptane) to give 2-(3-methyl-[1,2,4]oxadiazol-5-yl)-5-(4,4,5,5-tetramethyl-[1,3,2]dioxaborolan-2-yl)-indole-1-carboxylic acid *tert*-butyl ester **41** (2.8 g, 6.5 mmol, 71%). <sup>1</sup>H NMR (400 MHz, DMSO-*d*<sub>6</sub>): ppm 8.13 (s, 1H), 8.12 (d, *J* = 8.4 Hz, 1H), 7.80 (d, *J* = 9.3 Hz, 1H), 7.54 (s, 1H), 2.45 (s, 3H), 1.43 (s, 9H), 1.31 (s, 12H).

A reaction flask was charged with 4-[(5-bromo-1-methyl-1H-pyrazole-3-carbonyl)-amino]-methyl-benzoic acid (80 mg, 0.23 mmol), 2-(3-methyl-[1,2,4]oxadiazol-5-yl)-5-(4,4,5,5-tetramethyl-[1,3,2]dioxaborolan-2-yl)-indole-1-carboxylic acid *tert*-butyl ester **41** (110 mg, 0.26 mmol), bis(di-*tert*-butyl(4-dimethylaminophenyl)phosphine)dichloropalladium(II) (33 mg, 0.20 mmol), DMF (1.5 mL), and 2 M aqueous solution of sodium bicarbonate (0.38 mL, 0.775 mmol). The mixture was heated in a microwave reactor at 100 °C for 30 min, cooled to room temperature, diluted with EtOAc, and washed with water and brine. The organic layer was dried over anhydrous Na<sub>2</sub>SO<sub>4</sub>, filtered, and concentrated in vacuo. The resulting crude was purified by reversed-phase HPLC to give the title compound **11** (25 mg, 0.055 mmol, 23%) as a white solid. LCMS (ES+) *m/z* found, 457; retention time, 1.39 min. C<sub>24</sub>H<sub>20</sub>N<sub>6</sub>O<sub>4</sub> requires 457. HPLC: retention time, 8.1 min. <sup>1</sup>H NMR (400 MHz, DMSO-*d*<sub>6</sub>): ppm 12.86 (bs, 1H), 12.61 (s, 1H), 8.85 (t, *J* = 6.4 Hz, 1H), 7.91 (s, 2H), 7.89 (s, 1H), 7.61 (d, *J* = 8.4 Hz, 1H), 7.48 (dd, *J* = 8.4 Hz, 1.6 Hz, 1H), 7.44 (d, *J* = 1.6 Hz, 1H), 7.41 (d, *J* = 8.4 Hz, 2H), 6.77 (s, 1H), 4.50 (d, *J* = 6.4 Hz, 2H), 3.93 (s, 3H), 2.45 (s, 3H).

**4-[(1-Methyl-5-[2-(1-methyl-1H-pyrazol-4-yl)-1H-indol-5-yl]-1H-pyrazole-3-carbonyl)-amino]-methyl-benzoic Acid (12)**. The title compound was prepared according to the procedure described for **7** from 5-bromo-1-(*tert*-butoxycarbonyl)-1H-indol-2-yl-boronic acid **22** (500 mg, 1.47 mmol), 4-iodo-1-methyl-1H-pyrazole (305 mg, 1.47 mmol), bis(di-*tert*-butyl(4-dimethylaminophenyl)phosphine)dichloropalladium(II) (72 mg, 0.088 mmol), cesium carbonate (716 mg, 2.2 mmol), and 1,4-dioxane/water (13 mL/2 mL) to give 5-bromo-2-(1-methyl-1H-pyrazol-4-yl)-indole-1-carbox-

ylic acid *tert*-butyl ester **32** (227 mg, 41%). 5-Bromo-2-(1-methyl-1*H*-pyrazol-4-yl)-indole-1-carboxylic acid *tert*-butyl ester **32** (55 mg, 0.14 mmol), bis(pinacolato)diboron (75 mg, 0.29 mmol), bis-diphenylferrocenylpalladium(II)dichloride (36 mg, 0.044 mmol), potassium acetate (43 mg, 0.44 mmol), 1,4-dioxane (2 mL), 4-[(5-bromo-1-methyl-1*H*-pyrazole-3-carbonyl)-amino]-methyl}-benzoic acid (50 mg, 0.14 mmol), 2 N aqueous Na<sub>2</sub>CO<sub>3</sub> solution (0.16 mL, 0.32 mmol), and DMF (1 mL) were reacted to give 6-[5-(4-carboxy-benzylcarbamoyl)-2-methyl-2*H*-pyrazol-3-yl]-1-methyl-1*H*-pyrazol-4-yl-indole-1-carboxylic acid *tert*-butyl ester **37**, which was used for the next step without further purification. Deprotection of the BOC group with TFA yielded the title product **12** (18%). LCMS (ES<sup>+</sup>) *m/z* found, 455; retention time, 1.33 min. C<sub>25</sub>H<sub>22</sub>N<sub>6</sub>O<sub>3</sub> requires 455. HPLC: retention time, 8.4 min. <sup>1</sup>H NMR (400 MHz, DMSO-*d*<sub>6</sub>): ppm 12.51 (bs, 1H), 11.52 (s, 1H), 8.81 (t, *J* = 6.4 Hz, 1H), 8.13 (s, 1H), 7.91 (s, 2H), 7.89 (s, 1H), 7.62 (d, *J* = 1.2 Hz, 1H), 7.44 (d, *J* = 8.4 Hz, 1H), 7.41 (d, *J* = 8.4 Hz, 2H), 7.18 (dd, *J* = 8.4 Hz, 1.6 Hz, 1H), 6.70 (s, 1H), 6.62 (d, *J* = 1.2 Hz, 1H), 4.50 (d, *J* = 6.4 Hz, 2H), 3.91 (s, 3H), 3.90 (s, 3H).

**4-Methyl-4-[(4-methyl-5-[2-(3-methyl-[1,2,4]oxadiazol-5-yl)-1*H*-indol-5-yl]-1*H*-imidazole-2-carbonyl]-amino)-methyl]-benzoic Acid (**13**).** A flask was charged with 5-methyl-4-[2-(3-methyl-[1,2,4]oxadiazol-5-yl)-indol-6-yl]-1-(2-trimethylsilyl-ethoxymethyl)-1*H*-imidazole-2-carboxylic acid **49** (77 mg, 0.17 mmol) and DMF (1 mL). Diisopropylethylamine (0.125 mL, 0.67 mmol), 4-aminomethyl-benzoic acid ethyl ester hydrochloride (51 mg, 0.25 mmol), HATU (96 mg, 0.25 mmol), and HOAt (5 mg, 0.039 mmol) were added, and the resulting mixture was stirred at room temperature overnight. The reaction was diluted with EtOAc and washed with water and brine. The organic layer was dried over anhydrous Na<sub>2</sub>SO<sub>4</sub>, filtered, and concentrated in vacuo. The crude material was passed through a silica gel plug (EtOAc/hexane) to give 4-([5-methyl-4-[2,3-(3-methyl-[1,2,4]oxadiazol-5-yl)-1*H*-indol-6-yl]-1-(2-trimethylsilyl-ethoxymethyl)-1*H*-imidazole-2-carbonyl]-amino)-methyl)-benzoic acid methyl ester **52** (100 mg, 0.083 mmol, 98%), which was used without further purification. To a solution of 4-([5-methyl-4-[23(3-methyl-[1,2,4]oxadiazol-5-yl)-1*H*-indol-6-yl]-1-(2-trimethylsilyl-ethoxymethyl)-1*H*-imidazole-2-carbonyl]-amino)-methyl)-benzoic acid methyl ester **52** (100 mg, 0.083 mmol) in 1,4-dioxane (2.5 mL) was added 3 N HCl (2.5 mL, 7.5 mmol). The mixture was stirred at room temperature for 2.5 h, monitored by TLC. The solvent was evaporated and the residue was purified by reversed-phase HPLC to give the title compound **13** (23 mg, 60%). LCMS (ES<sup>+</sup>) *m/z* found, 457; retention time, 0.72 min. C<sub>24</sub>H<sub>20</sub>N<sub>6</sub>O<sub>4</sub> requires 457. HPLC: retention time, 8.39 min. <sup>1</sup>H NMR (400 MHz, DMSO-*d*<sub>6</sub>): ppm 12.42 (s, 1H), 12.1 (br s, 1H), 11.2 (br s, 1H), (9.03 (t, *J* = 6.4 Hz, 1H), 7.95 (s, 1H), 7.90 (d, *J* = 8.0 Hz, 2H), 7.67 (dd, *J* = 8.8 Hz, 1.6 Hz, 1H), 7.53 (d, *J* = 8.4 Hz, 1H), 7.44 (d, *J* = 8.4 Hz, 2H), 7.40 (d, *J* = 1.2 Hz, 1H), 4.54 (d, *J* = 6.4 Hz, 2H), 2.44 (s, 3H), 2.43 (s, 3H).

**4-Methyl-5-[2-(3-methyl-[1,2,4]oxadiazol-5-yl)-1*H*-indol-5-yl]-1*H*-imidazole-2-carboxylic Acid Amide (**14**).** To a suspension of 60% NaH in mineral oil (2.7 g, 67.5 mmol) in THF (100 mL) was added slowly a solution of 5-bromo-4-methyl-1*H*-imidazole **42** (10 g, 62.1 mmol) in THF (100 mL) over 20 min. The resulting mixture was stirred at room temperature for 1 h. The mixture was cooled to 0 °C, (2-chloromethoxy-ethyl)-trimethyl-silane (11 mL, 62.3 mmol) was added, and the reaction mixture was stirred at room temperature for another 2 h. The mixture was diluted with EtOAc and

washed with water and brine. The organic layer was dried over anhydrous Na<sub>2</sub>SO<sub>4</sub>, filtered, and concentrated in vacuo to give a mixture of two regioisomers: 5-bromo-4-methyl-1-(2-trimethylsilyl-ethoxymethyl)-1*H*-imidazole **43** and 4-bromo-5-methyl-1-(2-trimethylsilyl-ethoxymethyl)-1*H*-imidazole **44** as a yellow oil (17.6 g, 97%, approximately 1:1 ratio determined by <sup>1</sup>H NMR), which was carried to the next step without further purification.

A flask was charged with a mixture of 5-bromo-4-methyl-1-(2-trimethylsilyl-ethoxymethyl)-1*H*-imidazole and 4-bromo-5-methyl-1-(2-trimethylsilyl-ethoxymethyl)-1*H*-imidazole (**43** and **44**, respectively; 7.0 g, 24.0 mmol, 1:1 mole ratio) and THF (100 mL). The mixture was cooled to -78 °C, and a freshly prepared LDA solution (by mixing 1.6 N *n*-BuLi in hexane (21 mL, 33.6 mmol) with diisopropylamine (5.6 mL, 39.6 mmol) in THF (20 mL) at -10 °C for 30 min) was added at -78 °C. After stirring at -78 °C for 1 h, the solution was cannulated to a solution of ethyl chloroformate (4.5 mL, 47.2 mmol) in THF (25 mL) at -78 °C, and the resulting mixture was stirred at -78 °C for 30 min and then quenched with saturated NaHCO<sub>3</sub> solution. The mixture was diluted with EtOAc and washed with water and brine. The organic layer was dried over anhydrous Na<sub>2</sub>SO<sub>4</sub>, filtered, and concentrated in vacuo. The crude product was purified by chromatography over silica gel (EtOAc/hexane) to give 5-bromo-4-methyl-1-(2-trimethylsilyl-ethoxymethyl)-1*H*-imidazole-2-carboxylic acid ethyl ester **45** (2.0 g, 5.5 mmol, 23%) and 4-bromo-5-methyl-1-(2-trimethylsilyl-ethoxymethyl)-1*H*-imidazole-2-carboxylic acid ethyl ester **46** (3.2 g, 8.8 mmol, 36%).

To a solution of 4-bromo-5-methyl-1-(2-trimethylsilyl-ethoxymethyl)-1*H*-imidazole-2-carboxylic acid ethyl ester **46** (300 mg, 0.82 mmol) and 2-(3-methyl-[1,2,4]oxadiazol-5-yl)-5-(4,4,5,5-tetramethyl-[1,3,2]dioxaborolan-2-yl)-indole-1-carboxylic acid *tert*-butyl ester (300 mg, 0.75 mmol) in toluene (6 mL) was added 2 N aqueous Na<sub>2</sub>CO<sub>3</sub> solution (0.8 mL, 1.6 mmol). The resulting mixture was purged with argon, and bis(*di-tert*-butyl(4-dimethylaminophenyl)phosphine)-dichloropalladium(II) (75 mg, 0.10 mmol) was added. The mixture was heated at 110 °C for 12 h, then cooled to room temperature, diluted with EtOAc, and washed with water and brine. The organic layer was dried over anhydrous Na<sub>2</sub>SO<sub>4</sub>, filtered, and concentrated in vacuo. The crude product was purified by chromatography over silica gel (EtOAc/hexane) to give 6-[2-ethoxycarbonyl-5-methyl-1-(2-trimethylsilyl-ethoxymethyl)-1*H*-imidazol-4-yl]-2-(3-methyl-[1,2,4]oxadiazol-5-yl)-indole-1-carboxylic acid *tert*-butyl ester **47** (132 mg, 0.22 mmol, 32%), which was used without further purification.

A flask was charged with 6-[2-ethoxycarbonyl-5-methyl-1-(2-trimethylsilyl-ethoxymethyl)-1*H*-imidazol-4-yl]-2-(3-methyl-[1,2,4]oxadiazol-5-yl)-indole-1-carboxylic acid *tert*-butyl ester **47** (105 mg, 0.18 mmol) and THF/MeOH (2 mL/2 mL), and 1 N solution of sodium hydroxide (0.4 mL, 0.40 mmol) was added. The reaction was stirred at room temperature for 8 h, then additional water was added, and the mixture was acidified to pH 4–5 with 1 N HCl. The precipitates were collected by filtration and washed with water. The resulting solid was dried in an oven at 60 °C for 16 h to give 5-methyl-4-[2-(3-methyl-[1,2,4]oxadiazol-5-yl)-indol-6-yl]-1-(2-trimethylsilyl-ethoxymethyl)-1*H*-imidazole-2-carboxylic acid **48** (60 mg, 0.13 mmol, 73%) as a white solid.

To a solution of 5-methyl-4-[2-(3-methyl-[1,2,4]oxadiazol-5-yl)-indol-6-yl]-1-(2-trimethylsilyl-ethoxymethyl)-1*H*-imidazole-2-carboxylic acid **48** (40 mg, 0.06 mmol) in DMF (3 mL)

was added 1-ethyl-3-(3-dimethylaminopropyl)carbodiimide hydrochloride (30 mg, 0.15 mmol) followed by HOBT (25 mg, 0.16 mmol). The mixture was stirred at room temperature for 1 h. Ammonium hydroxide (28%, 0.2 mL, 1.59 mmol) was added, and the resulting mixture was stirred for 16 h, then diluted with EtOAc, and washed with water and brine. The organic layer was dried over anhydrous Na<sub>2</sub>SO<sub>4</sub>, filtered, and concentrated in vacuo. The resulting crude product was purified by chromatography over silica gel (EtOAc/hexane) to give 5-methyl-4-[2-(3-methyl-[1,2,4]oxadiazol-5-yl)-indol-6-yl]-1-(2-trimethylsilyl-ethoxymethyl)-1H-imidazole-2-carboxylic acid amide **49** (23 mg, 0.05 mmol, 82%). <sup>1</sup>H NMR (400 MHz, DMSO-*d*<sub>6</sub>): ppm 9.19 (s, 1H), 7.93 (s, 1H), 7.72 (dd, *J* = 8.8 Hz, 1.6 Hz, 1H), 7.60 (s, 1H), 7.45 (d, *J* = 8.8 Hz, 1H), 7.39 (d, *J* = 1.6 Hz, 1H), 7.25 (s, 1H), 5.27 (s, 2H), 3.54 (t, *J* = 8.4 Hz, 2H), 2.46 (s, 3H), 0.93 (t, *J* = 8.4 Hz, 2H), 0.001 (9H).

To a solution of 5-methyl-4-[2-(3-methyl-[1,2,4]oxadiazol-5-yl)-indol-6-yl]-1-(2-trimethylsilyl-ethoxymethyl)-1H-imidazole-2-carboxylic acid amide **49** (21 mg, 0.046 mmol) in ethanol (2 mL) was added 3 N HCl (1 mL, 3 mmol). The mixture was heated to 100 °C for 4 h. The reaction was cooled to room temperature, and the gray precipitates were collected by filtration, washed with 60% aqueous ethanol, and dried to give 5-methyl-4-[2-(3-methyl-[1,2,4]oxadiazol-5-yl)-indol-6-yl]-1H-imidazole-2-carboxylic acid amide **14** (14 mg, 0.039 mmol, 84%). LCMS (ES+) *m/z* found, 323; retention time, 0.58 min. C<sub>16</sub>H<sub>14</sub>N<sub>6</sub>O<sub>2</sub> requires 323. HPLC: retention time, 7.03 min. <sup>1</sup>H NMR (400 MHz, DMSO-*d*<sub>6</sub>): ppm 12.58 (s, 1H), 11.1 (bs 1H), 8.35 (bs, 1H), 8.15 (bs, 1H), 8.01 (s, 1H), 7.65 (dd, *J* = 8.8 Hz, 1.6 Hz, 1H), 7.60 (d, *J* = 8.8 Hz, 1H), 7.45 (d, *J* = 1.6 Hz, 1H), 2.47 (s, 3H), 2.44 (s, 3H).

**4-Methyl-5-[2-(3-methyl-[1,2,4]oxadiazol-5-yl)-1H-indol-5-yl]-1H-imidazole-2-carboxylic Acid Ethylamide (15).** The title compound was prepared according to the procedure described for **14** from 5-methyl-4-[2-(3-methyl-[1,2,4]oxadiazol-5-yl)-indol-6-yl]-1-(2-trimethylsilyl-ethoxymethyl)-1H-imidazole-2-carboxylic acid (40 mg, 0.06 mmol), DMF (3 mL), 1-ethyl-3-(3-dimethylaminopropyl)carbodiimide hydrochloride (30 mg, 0.15 mmol), HOBT (20 mg, 0.13 mmol), and 70% aqueous ethyl amine (0.2 mL, 2.48 mmol) to give 5-methyl-4-[2-(3-methyl-[1,2,4]oxadiazol-5-yl)-indol-6-yl]-1-(2-trimethylsilyl-ethoxymethyl)-1H-imidazole-2-carboxylic acid ethylamide **50** (24 mg, 0.05 mmol, 73%).

To a solution of 5-methyl-4-[2-(3-methyl-[1,2,4]oxadiazol-5-yl)-indol-6-yl]-1-(2-trimethylsilyl-ethoxymethyl)-1H-imidazole-2-carboxylic acid ethylamide **50** (21 mg, 0.044 mmol) in ethanol (2 mL) was added 6 N HCl (1 mL, 6 mmol). The mixture was heated to 100 °C for 7 h. The reaction mixture was cooled to room temperature, and the gray precipitates were collected by filtration, washed with 60% aqueous ethanol, and dried to give the title compound **15** (14 mg, 0.037 mmol, 86%). LCMS (ES+) *m/z* found, 351; retention time, 0.69 min. C<sub>18</sub>H<sub>18</sub>N<sub>6</sub>O<sub>2</sub> requires 351. HPLC: retention time, 7.69 min. <sup>1</sup>H NMR (400 MHz, DMSO-*d*<sub>6</sub>): ppm 12.51 (s, 1H), 11.21 (bs 1H), 8.70 (bs, 1H), 7.98 (s, 1H), 7.66 (dd, *J* = 8.8 Hz, 1.6 Hz, 1H), 7.56 (d, *J* = 8.8 Hz, 1H), 7.43 (d, *J* = 1.6 Hz, 1H), 3.33 (m, 2H), 2.45 (s, 3H), 2.44 (s, 3H), 1.15 (t, *J* = 7.2 Hz, 3H).

**4-Methyl-5-[2-(3-methyl-[1,2,4]oxadiazol-5-yl)-1H-indol-5-yl]-1H-imidazole-2-carboxylic Acid (Tetrahydropyran-4-ylmethyl)-amide (16).** A flask was charged with 6-[2-ethoxycarbonyl-5-methyl-1-(2-trimethylsilyl-ethoxymethyl)-1H-imidazol-4-yl]-2-(3-methyl-[1,2,4]oxadiazol-5-yl)-indole-1-carboxylic acid *tert*-butyl ester **47** (2.9 g, 4.4 mmol), TFA

(10 mL), and CH<sub>2</sub>Cl<sub>2</sub> (5 mL). The mixture was stirred at room temperature for 3 h. The solvent was evaporated in vacuo to give 5-methyl-4-[2-(3-methyl-[1,2,4]oxadiazol-5-yl)-1H-indol-6-yl]-1H-imidazole-2-carboxylic acid ethyl ester **51** (1.5 g, 4.4 mmol, 100%), which was used for the following step without further purification.

To a solution of 5-methyl-4-[2-(3-methyl-[1,2,4]oxadiazol-5-yl)-1H-indol-6-yl]-1H-imidazole-2-carboxylic acid ethyl ester **51** (1.5 g, 4.4 mmol) in THF/water (100 mL, 3:2 v:v) was added LiOH (0.33 g, 8.9 mmol). The reaction mixture was stirred at room temperature for 16 h. The solvent was evaporated in vacuo and the residue was dried under high vacuum for 16 h. The residue was suspended in DCM (100 mL), and MeOH (20 mL) was added. The solution was filtered through a short silica column and washed several times with MeOH. The solvent was removed in vacuo to give 5-methyl-4-[2-(3-methyl-[1,2,4]oxadiazol-5-yl)-1H-indol-6-yl]-1H-imidazole-2-carboxylic acid **52** (2.2 g, 6.8 mmol, 151%) as a pale yellow solid, which was used for the following step without further purification.

A flask was charged with 5-methyl-4-[2-(3-methyl-[1,2,4]oxadiazol-5-yl)-1H-indol-6-yl]-1H-imidazole-2-carboxylic acid (50 mg, 0.15 mmol) and DMF (1 mL). Diisopropylethylamine (0.05 mL, 0.31 mmol), 4-aminomethyltetrahydropyran (26 mg, 0.23 mmol), HATU (88 mg, 0.23 mmol), and HOAt (5 mg, 0.039 mmol) were subsequently added. The resulting mixture was stirred at room temperature for 4 h. The solvent was removed and the residue was purified by reversed-phase HPLC to give 4-methyl-5-[2-(3-methyl-[1,2,4]oxadiazol-5-yl)-1H-indol-5-yl]-1H-imidazole-2-carboxylic acid (tetrahydropyran-4-ylmethyl)-amide **16** (10 mg, 0.024 mmol, 15%) as a beige solid. LCMS (ES+) *m/z* found, 421; retention time, 0.72 min. C<sub>22</sub>H<sub>24</sub>N<sub>6</sub>O<sub>3</sub> requires 421. HPLC: retention time, 8.08 min. <sup>1</sup>H NMR (400 MHz, MeOH-*d*<sub>4</sub>): ppm 7.98 (d, *J* = 1.2 Hz, 1H), 7.70 (d, *J* = 8.8 Hz, 1H), 7.55 (dd, *J* = 8.8 Hz, 1.6 Hz, 1H), 7.46 (s, 1H), 3.98 (dm, *J* = 11.2 Hz, 2H), 3.44 (td, *J* = 12 Hz, 2.0 Hz, 2H), 3.39 (d, *J* = 6.8 Hz, 2H), 2.55 (s, 3H), 2.47 (s, 3H), 1.95 (m, 1H), 1.75 (dm, *J* = 12.8 Hz, 2H), 1.40 (td, *J* = 12 Hz, 4.4 Hz, 2H).

**4-Methyl-5-[2-(3-methyl-[1,2,4]oxadiazol-5-yl)-1H-indol-5-yl]-1H-imidazole-2-carboxylic Acid (Pyridin-4-ylmethyl)-amide (17).** The title compound was prepared according to the procedure described for **13** from 5-methyl-4-[2-(3-methyl-[1,2,4]oxadiazol-5-yl)-indol-6-yl]-1-(2-trimethylsilyl-ethoxymethyl)-1H-imidazole-2-carboxylic acid **49** (40 mg, 0.088 mmol), DMF (1 mL), diisopropylethylamine (40 mg, 0.31 mmol), 4-(aminomethyl)pyridine (15 mg, 0.14 mmol), HATU (60 mg, 0.16 mmol), and HOAt (15 mg, 0.11 mmol) to give 4-[methyl-4-(3-methyl-[1,2,4]oxadiazol-5-yl)-1H-indol-6-yl]-1-(2-trimethylsilyl-ethoxymethyl)-1H-imidazole-2-carboxylic acid (pyridine-4-ylmethyl)-amide **53** (45 mg, 0.083 mmol, 94%), which was used for the next step without further purification.

To a solution of 4-[methyl-4-(3-methyl-[1,2,4]oxadiazol-5-yl)-1H-indol-6-yl]-1-(2-trimethylsilyl-ethoxymethyl)-1H-imidazole-2-carboxylic acid (pyridine-4-ylmethyl)-amide **53** (45 mg, 0.083 mmol) in EtOH (2 mL) was added 6 N HCl (1 mL, 6 mmol). The mixture was heated to 100 °C for 7 h. The reaction was cooled to room temperature and basified by 3 N NaOH to pH 8–9. The yellow precipitates were collected by filtration and further purified by reversed-phase HPLC to give the title compound **17** (25 mg, 0.06 mmol, 73%). LCMS (ES+) *m/z* found, 414; retention time, 0.53 min. C<sub>22</sub>H<sub>19</sub>N<sub>7</sub>O<sub>2</sub> requires 413. HPLC: retention time, 7.08 min. <sup>1</sup>H NMR (400 MHz, DMSO-

$d_6$ ): ppm 12.42 (s, 1H), 11.01 (bs, 1H), 9.20 (t,  $J = 6.4$  Hz, 1H), 8.78 (d,  $J = 6.8$  Hz, 2H), 7.97 (s, 1H), 7.83 (d,  $J = 6.4$  Hz, 2H), 7.70 (dd,  $J = 8.8$  Hz, 1.6 Hz, 1H), 7.53 (d,  $J = 8.8$  Hz, 1H), 7.40 (d,  $J = 1.2$  Hz, 1H), 4.69 (d,  $J = 6.4$  Hz, 2H), 2.45 (s, 3H), 2.44 (s, 3H).

**4-Methyl-5-[2-(3-methyl-[1,2,4]oxadiazol-5-yl)-1H-indol-5-yl]-1H-imidazole-2-carboxylic Acid (Pyridin-3-ylmethyl)-amide (18).** The title compound was prepared according to the procedure described for **13** from 5-methyl-4-[2-(3-methyl-[1,2,4]oxadiazol-5-yl)-indol-6-yl]-1-(2-trimethylsilylanyl-ethoxymethyl)-1H-imidazole-2-carboxylic acid **49** (75 mg, 0.165 mmol), DMF (2 mL), diisopropylethylamine (0.059 mL, 0.34 mmol), 3-(aminomethyl)pyridine (36 mg, 0.34 mmol), HATU (66 mg, 0.17 mmol), and HOAt (6.0 mg, 0.045 mmol) to give 4-[methyl-4-(3-methyl-[1,2,4]oxadiazol-5-yl)-1H-indol-6-yl]-1-(2-trimethylsilylanyl-ethoxymethyl)-1H-imidazole-2-carboxylic acid (pyridine-3-ylmethyl)-amide **54** (35 mg, 0.065 mmol, 39%), which was purified by reversed-phase HPLC.

To a solution of 4-[methyl-4-(3-methyl-[1,2,4]oxadiazol-5-yl)-1H-indol-6-yl]-1-(2-trimethylsilylanyl-ethoxymethyl)-1H-imidazole-2-carboxylic acid (pyridine-3-ylmethyl)-amide **54** (35 mg, 0.065 mmol) in  $\text{CH}_2\text{Cl}_2$  (1 mL) was added TFA (0.5 mL). The reaction was stirred at room temperature for 3 h and then concentrated in vacuo. The residue was purified by reversed-phase HPLC to give the title compound **18** (3 mg, 0.007 mmol, 11%). LCMS (ES+)  $m/z$  found, 414; retention time, 0.55 min.  $\text{C}_{22}\text{H}_{19}\text{N}_7\text{O}_2$  requires 413. HPLC: retention time, 7.14 min.  $^1\text{H}$  NMR (400 MHz,  $\text{DMSO}-d_6$ ): ppm 12.42 (s, 1H), 10.9 (bs 1H) 9.11 (t,  $J = 6.4$  Hz, 1H), 8.75 (s, 1H), 8.67 (d,  $J = 4.8$  Hz, 1H), 8.19 (d,  $J = 6.8$  Hz, 1H), 7.95 (s, 1H), 7.75 (s, 1H), 7.68 (d,  $J = 8.4$  Hz, 1H), 7.52 (d,  $J = 8.8$  Hz, 1H), 7.40 (d,  $J = 2.0$  Hz, 1H), 4.59 (d,  $J = 6.4$  Hz, 2H), 2.44 (s, 6H).

**4-Methyl-5-[2-(3-methyl-[1,2,4]oxadiazol-5-yl)-1H-indol-5-yl]-1H-imidazole-2-carboxylic Acid (Pyridin-2-ylmethyl)-amide (19).** The title compound was prepared according to the procedure described for **16** from 5-methyl-4-[2-(3-methyl-[1,2,4]oxadiazol-5-yl)-1H-indol-6-yl]-1H-imidazole-2-carboxylic acid (75 mg, 0.23 mmol), DMF (1 mL), diisopropylethylamine (0.08 mL, 0.46 mmol), 2-aminomethylpyridine (0.036 mL, 0.34 mmol), HATU (132 mg, 0.34 mmol), and HOAt (8 mg, 0.058 mmol) to give the title compound **19** (5 mg, 0.012 mmol, 5%). LCMS (ES+)  $m/z$  found, 414; retention time, 1.13 min.  $\text{C}_{22}\text{H}_{19}\text{N}_7\text{O}_2$  requires 413. HPLC: retention time, 7.5 min.  $^1\text{H}$  NMR (400 MHz,  $\text{DMSO}-d_6$ ): ppm 12.42 (s, 1H), 11.2 (s, 1H), 9.00 (t,  $J = 6.4$  Hz, 1H), 8.61 (d,  $J = 4.8$  Hz, 1H), 7.97 (s, 1H), 7.70 (dd,  $J = 8.8$  Hz, 1.6 Hz, 1H), 7.44–7.60 (m, 4H), 7.41 (d,  $J = 2.0$  Hz, 1H), 4.65 (d,  $J = 6.4$  Hz, 2H), 2.45 (s, 3H), 2.44 (s, 3H).

**4-Methyl-5-[2-(3-methyl-[1,2,4]oxadiazol-5-yl)-1H-indol-5-yl]-1H-imidazole-2-carboxylic Acid (6-Oxo-1,6-dihydro-pyridin-3-ylmethyl)-amide (20).** The title compound was prepared according to the procedure described for **13** from 5-methyl-4-[2-(3-methyl-[1,2,4]oxadiazol-5-yl)-indol-6-yl]-1-(2-trimethylsilylanyl-ethoxymethyl)-1H-imidazole-2-carboxylic acid **49** (50 mg, 0.11 mmol), DMF (1 mL), diisopropylethylamine (0.1 mL, 0.54 mmol), 5-aminomethyl-1H-pyridin-2-one (20 mg, 0.16 mmol), and HATU (62 mg, 0.16 mmol) to give 4-[methyl-4-(3-methyl-[1,2,4]oxadiazol-5-yl)-1H-indol-6-yl]-1-(2-trimethylsilylanyl-ethoxymethyl)-1H-imidazole-2-carboxylic acid (1H-pyridin-2-one-5-ylmethyl)-amide **55** (56 mg, 90%), which was purified by chromatography in silica gel ( $\text{MeOH}/\text{CH}_2\text{Cl}_2$ ).

To a solution of 4-[methyl-4-(3-methyl-[1,2,4]oxadiazol-5-yl)-1H-indol-6-yl]-1-(2-trimethylsilylanyl-ethoxymethyl)-1H-imidazole-2-carboxylic acid (1H-pyridin-2-one-5-ylmethyl)-amide **55** (56 mg, 0.10 mmol) in 1,4-dioxane (2.5 mL) was added 3 N HCl (2.5 mL, 7.5 mmol). The mixture was heated to 100 °C for 1 h. The reaction mixture was concentrated, and the residue was purified by reversed-phase HPLC to give the title compound **20** (15 mg, 35%). LCMS (ES+)  $m/z$  found, 430; retention time, 1.15 min.  $\text{C}_{22}\text{H}_{19}\text{N}_7\text{O}_3$  requires 430. HPLC: retention time, 8.2 min.  $^1\text{H}$  NMR (400 MHz,  $\text{DMSO}-d_6$ ): ppm 12.36 (s, 1H), 11.42 (bs, 1H), 11.1 (bs 1H), 8.74 (t,  $J = 6.4$  Hz, 1H), 7.95 (s, 1H), 7.71 (dd,  $J = 8.4$  Hz, 1.2 Hz, 1H), 7.50 (d,  $J = 8.8$  Hz, 1H), 7.46 (dd,  $J = 9.2$  Hz, 2.0 Hz, 1H), 7.38 (s, 1H), 7.26 (s, 1H), 7.30 (d,  $J = 9.6$  Hz, 1H), 4.17 (d,  $J = 6.4$  Hz, 2H), 2.44 (s, 3H), 2.43 (s, 3H).

**4-Methyl-5-[2-(3-methyl-[1,2,4]oxadiazol-5-yl)-1H-indol-5-yl]-1H-imidazole-2-carboxylic Acid Benzylamide (21).** The title compound was prepared according to the procedure described for **13** from 5-methyl-4-[2-(3-methyl-[1,2,4]oxadiazol-5-yl)-indol-6-yl]-1-(2-trimethylsilylanyl-ethoxymethyl)-1H-imidazole-2-carboxylic acid **49** (78 mg, 0.16 mmol), DMF (2 mL), diisopropylethylamine (0.13 mL, 0.65 mmol), benzylamine (19 mg, 0.18 mmol), and HATU (91 mg, 0.24 mmol) to give 4-[methyl-4-(3-methyl-[1,2,4]oxadiazol-5-yl)-1H-indol-6-yl]-1-(2-trimethylsilylanyl-ethoxymethyl)-1H-imidazole-2-carboxylic acid benzylamide **56** (89 mg, 100%), which was used for the next step without further purification.

To a solution of 4-[methyl-4-(3-methyl-[1,2,4]oxadiazol-5-yl)-1H-indol-6-yl]-1-(2-trimethylsilylanyl-ethoxymethyl)-1H-imidazole-2-carboxylic acid benzylamide **56** (89 mg, 0.16 mmol) in 1,4-dioxane (1 mL) was added 3 N HCl (1 mL, 3 mmol). The mixture was heated to 100 °C for 1 h. The reaction was concentrated, and the residue was purified by reversed-phase HPLC to give the title compound **21** (8 mg, 0.02 mmol, 12%). LCMS (ES+)  $m/z$  found, 413; retention time, 0.86 min.  $\text{C}_{23}\text{H}_{20}\text{N}_6\text{O}_2$  requires 412. HPLC: retention time, 9.44 min.  $^1\text{H}$  NMR (400 MHz,  $\text{DMSO}-d_6$ ): ppm 12.35 (s, 1H), 11.2 (s, 1H), 8.82 (t,  $J = 6.0$  Hz, 1H), 7.94 (s, 1H), 7.68 (bs, 1H), 7.50 (d,  $J = 8.4$  Hz, 1H), 7.38 (d,  $J = 1.2$  Hz, 1H), 7.31–7.33 (m, 4H), 7.23 (m, 1H), 4.46 (d,  $J = 6.4$  Hz, 2H), 2.43 (s, 6H).

## CRYSTALLOGRAPHY

Experiments were run similarly to ref 11. A fragment of human MMP-13 corresponding to residues 104–274 was expressed using the pET29a vector system (Invitrogen) and *Escherichia coli* BL21(DE3) as the host strain. The protein was expressed in an insoluble form. Cell pellets were lysed at 4 °C using five, 1 min cycles of sonication in a buffer containing 50 mM MES, 75 mM NaCl, and 0.5% Triton at pH 6.5. Following sonication, the pellet was recovered by centrifugation, and the supernatant was decanted. This sonication process and pellet recovery were repeated three times, with the final pellet containing the inclusion bodies frozen at –80 °C. The pellet containing the inclusion bodies was thawed and resolubilized in buffer at room temperature (6 M urea and 150 mM MES, pH 6.5). Inhibition of protease activity was accomplished through the addition of Complete protease inhibitor cocktails (Roche). The resuspended material was clarified using centrifugation, and the supernatant was separated and stored. The supernatant was dialyzed against a buffer containing 6 M urea and 50 mM MES (pH 6.5). The dialyzed material was then purified using an SP Sepharose Fast Flow resin (GE Life Sciences). Separation was achieved using a buffer containing 6 M urea and 50 mM MES

(pH 6.5) and a 0–250 mM NaCl gradient. Fractions containing the MMP-13 protein were pooled and stored at  $-80\text{ }^{\circ}\text{C}$ . The protein was refolded using sequential dialysis of the protein (at a concentration of 0.25 mg/mL) against a buffer containing 50 mM MES (pH 6.5), 500 mM NaCl, 10 mM  $\text{CaCl}_2$ , 1.0 mM  $\text{ZnCl}_2$ , and urea. The urea concentration was reduced in the following steps, 4, 2, 1, 0, and 0 M, over approximately 2 days. The dialyzed protein was then concentrated to  $\sim 13\text{ mg/mL}$ , and purification and buffer exchange were achieved via SEC on a Superex75 resin (GE Life Sciences) with a running buffer of 50 mM Tris (pH 8.0), 150 mM NaCl, and 5 mM  $\text{CaCl}_2$ . The fractions corresponding to MMP-13 were pooled and concentrated to 7 mg/mL. A 2-fold excess of compound **1** was added to the protein, and crystals were obtained using a hanging drop method with a precipitant containing 10% w/v PEG4000, 1 M ammonium formate, and 100 mM Tris (pH 8.0). Crystals with compounds **11** and **15** were generated by soaking out crystals containing compound **1**. X-ray diffraction data were collected using either a Rigaku FR-E SuperBright generator and a Saturn92 CCD detector or the PX1 beamline at the SwissLight Source. Data reduction was achieved using HKL2000. An initial overall structure was obtained via molecular replacement using available coordinates of MMP-13 (PDB code: 1XUD) as a starting model. Numerous rounds of refinement were performed using Phenix. The costructure of MMP-13 with compound **1** had a resolution of 2.00 Å and R/Rfree statistics of 0.20/0.26.

## ■ BIOLOGICAL ASSAYS

**Biochemical/ Molecular MMP Assays (Human, Murine, and Other Isoforms).** Experiments were run similarly to ref 11.

Catalytic domains of human MMP-13 were expressed and purified from *E. coli* in-house. MMP-13 was assayed in a 20  $\mu\text{L}$  volume containing a 125 pM catalytic domain of human MMP13 and 2  $\mu\text{M}$  520 MMP FRET Substrate XIV [sequence: QXL520-GABA-Pro-Cha-Abu-Smc-His-Ala-Dab(5-FAM)-Ala\_Lys-NH2] (Anaspec) in a buffer containing 100 mM Tris-HCl (pH 7.5), 100 mM NaCl, 10 mM  $\text{CaCl}_2$ , 0.05% BRIJ 35, and 1% DMSO for 30 min at 28  $^{\circ}\text{C}$ /80% humidity, and fluorescence was read at 485 nm excitation and 535 nm emission. All other MMPs were assayed as described for MMP-13 with enzyme substitutions as follows: 4 nM catalytic domain of recombinant human MMP-1(Biomol), 2 nM catalytic domain of recombinant human MMP-2 (Biomol), 0.8 nM catalytic domain of recombinant human MMP-3 (Biomol), 0.6 nM catalytic domain of recombinant human MMP-7 (Biomol), 2 nM catalytic domain of recombinant human MMP-8 (Biomol), 1.5 nM catalytic domain of recombinant human MMP-9 (Biomol), 1 nM catalytic domain of recombinant human MMP-10 (Biomol), and 0.125 nM catalytic domain of recombinant human MMP-12 (Biomol). MMP-14 was assayed as described for MMP-13 with an enzyme exchange of 8.8 nM catalytic domain of recombinant human MMP-14 (Biomol) and an extended linear incubation time of 60 min at 28  $^{\circ}\text{C}$ /80% humidity. MMP-13 with 1.25% human serum was assayed as described for MMP-13 with the addition of 1.25% human serum to the assay buffer.

**Collagen Degradation Assay.** Experiments were run similarly to ref 11.

For the collagen degradation assay (full-length MMP-13  $\text{IC}_{50}$ ), the Rapid Collagen Assay kit by Condrex (catalog #3002) was applied to measure the activity of MMP-13 in degrading FITC-labeled collagen II. Full-length MMP-13 was activated by 1 mM AMPA, and the activated FL-MMP13 (600 ng/mL) was

incubated with FITC-labeled type II collagen in the kit assay buffer for 1.5 h at 37  $^{\circ}\text{C}$ . The degraded collagen sections were extracted into solution and assessed by the fluorescence intensity of FITC (490 nm excitation/520 nm emission) as depicted in the assay kit protocol ([https://www.chondrex.com/documents/Collagenase\\_Kit.pdf](https://www.chondrex.com/documents/Collagenase_Kit.pdf)).  $\text{IC}_{50}$  values are determined by nonlinear curve fitting of the data from a duplicate 10-point concentration–response curve. The bovine nasal cartilage (BNC) degradation assay measures the ability of compounds to inhibit full-length MMP-13-induced cartilage degradation. BNC explants were purchased from Northland Laboratories ([www.northlandlabs.com](http://www.northlandlabs.com)) as 3 mm explants in 96-well plates. The BNC explants were washed with PBS and cultured with activated full-length human MMP-13 (50  $\mu\text{g/mL}$ ) (Biomol) in the assay buffer containing 50 mM Tris (pH 6.5), 250 mM NaCl, 5 mM  $\text{CaCl}_2$ , 1  $\mu\text{M}$   $\text{ZnCl}_2$ , and 10% human serum for 2 h at 37  $^{\circ}\text{C}$ . The cartilage degradation product C-terminal telopeptide of type II collagen (CTXII) was quantified by an CTXII ELISA (IDS, formerly Nordic Bioscience, catalog #3CAL4000) using the cartilage culture supernatants. Test compound  $\text{EC}_{50}$  values are determined by nonlinear curve fitting of the data from a duplicate 8-point concentration–response curve.

**hLM (Human Liver Microsome Stability Assay).** Experiments were run similarly to ref 11.

The data collected were analyzed to calculate the half-life ( $t_{1/2}$ , min) for test compounds. The assay was performed in 50 mM potassium phosphate buffer (pH 7.4) and 2.5 mM NADPH. Test samples were dissolved in acetonitrile for a final assay concentration of 1–10  $\mu\text{M}$ . Human liver microsomes were diluted in assay buffer to a final assay concentration of 1 mg protein/mL. A volume of 25  $\mu\text{L}$  of compound solution and 50  $\mu\text{L}$  of microsome suspension were added to 825  $\mu\text{L}$  of assay buffer. The preparation was incubated for 5 min in a 37  $^{\circ}\text{C}$  water bath. The addition of 100  $\mu\text{L}$  of NADPH started the reaction. Volumes of 80  $\mu\text{L}$  were removed at 0 and 15 or 30 min and added to 160  $\mu\text{L}$  of acetonitrile. The samples were shaken for 20 s and then centrifuged for 3 min at 3000 rpm. A 200  $\mu\text{L}$  volume of the supernatant was transferred to 0.25 mm glass fiber filter plates and centrifuged for 5 min at 3000 rpm. Injection volumes of 10  $\mu\text{L}$  were typically added to Zorbax SB C8 HPLC columns with formic acid in water or acetonitrile at a 1.5 mL/min flow rate. The percent loss of the parent compound was calculated from the area under each time point to determine the half-life, which was then converted relative to hepatic blood flow.

**Aqueous Solubility.** Experiments were run similarly to ref 11.

For the preparation of a reference UV plate, 10  $\mu\text{L}$  of each stock sample (including DMSO control) was added to 190  $\mu\text{L}$  of propanol to prepare the reference stock plate. After reading spectrophotometrically, reference stock samples were mixed and 5  $\mu\text{L}$  of each stock sample was added to the UV blank plate. For the sample preparation, 5  $\mu\text{L}$  of each sample (including DMSO control) was added to the deep well plate containing 1000  $\mu\text{L}$  of pH 7.4 buffer, mixed, and incubated for 16–19 h. The plate was sealed well during the incubation process. At the end of the incubation period, 100  $\mu\text{L}$  of the sample from the deep well plate was vacuum-filtered using a filter plate. Another 200  $\mu\text{L}$  of the sample from the deep well plate was vacuum-filtered using the same filter block but a clean filter plate. Seventy-five microliters of the filtrate from the filter plate was transferred to a UV sample plate. Seventy-two microliters of propanol was added to this UV plate. The solution was mixed and the spectrum was read using

the UV spectrophotometer. For data analysis, the spectra collected for the blank, reference, and sample from 250 to 498 nm were analyzed using pION software.

**Caco-2.** Experiments were run similarly to ref 11.

Caco-2 cells were maintained at 37 °C in complete Dulbecco's modified Eagle's medium, containing 10% fetal bovine serum, 1.1% non-essential amino acids, 100 units/mL penicillin, and 100 mg/mL streptomycin, in an atmosphere of 5% CO<sub>2</sub> and 90% relative humidity. Cells grown in 175 cm<sup>2</sup> T-flasks were passaged every 7 days. For permeability experiments, cells were seeded at a density of 80,000 cells/cm<sup>2</sup> in Costar 12-well plates on Transwell polycarbonate filters (12 mm in diameter, with a 0.4 mm pore size). The medium (0.5 mL in the insert and 1.0 mL in the well) was changed every other day for the first 7 days and every day thereafter. The cells were allowed to grow and differentiate for 21 to 25 days. The culture medium was aspirated from monolayers prior to the experiment. Hank's Balanced Salt Solution (1×, pH 7.4) was added to both the inserts (0.5 mL) and the wells (1.0 mL), allowed to equilibrate at 37 °C for 30 min, and then removed. A dosing solution of the test compound was prepared in 1× Hank's Balanced Salt Solution (pH 7.4) at a nominal concentration of 50 mM. The dosing solution was then allowed to equilibrate overnight at room temperature while being mixed on a magnetic stirrer. Prior to the experiment, the dosing solution was filtered through a 0.45 mm PVDF filter to remove any insoluble substances. The actual concentration of the dosing solution was represented by the peak area during the data analysis. For the experiment, the dosing solution was added to the donor side of the monolayers, the apical side for an A/B experiment, and the basolateral side for a B/A experiment. Hank's Balanced Salt Solution (1×; pH 7.4) was added to the receiver side of the monolayers. At each time point, samples were collected from the receiver side of the monolayers. Both AB and BA experiments were conducted in duplicate, and samples were collected at 15, 30, 60, 90, 120, and 150 min. The analysis was done by LC/MS/MS, and the permeability coefficients (cm/s) were determined.

**In Vivo Pharmacokinetics.** Experiments were run similarly to ref 11.

Compounds were tested in Sprague Dawley rats ( $N = 3$ ) by intravenous injection (1 mpk, 70% PEG) or oral gavage as a suspension (10 mpk, methylcellulose). The compound was administered intravenously to rats, and blood samples were taken at various time points post dose. The blood samples were anticoagulated and centrifuged to recover plasma, which was then analyzed to quantify concentrations of the parent compound. PK parameters were calculated using noncompartmental methods. The compound was administered orally to rats, and blood samples were taken at various time points post dose. The blood samples were anticoagulated and centrifuged to recover plasma, which was then analyzed to quantify concentrations of the parent compound. PK parameters were calculated using noncompartmental methods.

**Collagen Antibody-Induced Arthritis (CAIA).** All animal experiments performed in the paper were conducted in compliance with institutional guidelines. Chronic inflammatory arthritis was induced in 8–10 week-old female B10.RIII mice (The Jackson Laboratory) by intraperitoneal injection of 2 mg (200  $\mu$ L) of arthritogenic anti-collagen type II monoclonal antibody cocktail (Chemicon), followed 3 days later by intraperitoneal injection with 37.5  $\mu$ g of LPS. Beginning on day 4, mice were treated twice daily by oral gavage with compounds (100 mg/kg) or 1% critical micelle concentration

(CMC), 0.015% Tween 80 (10 mL/kg) vehicle control. Arthritic severity and disease progression were monitored daily using a visual scoring system from days 3 to 14. Each limb was graded as follows: 0 = normal; 1 = edema in 1–2 digits; 2 = edema in >2 digits or mild edema about the tibio-tarsal joint; 3 = moderate edema to include the metatarsals; 4 = maximal edema to include the metatarsals and phalanges. The clinical score per paw was summed to give a maximal severity score of 16 for each animal. Body mass was monitored three times per week.

## ■ AUTHOR INFORMATION

### Corresponding Author

Steven J. Taylor – Boehringer Ingelheim Pharmaceuticals Inc., Ridgefield, Connecticut 06877-0368, United States; Present Address: Skyhawk Therapeutics, 35 Gatehouse Drive, Waltham, Massachusetts 02451, United States (S.J.T.); [orcid.org/0000-0002-0450-5036](https://orcid.org/0000-0002-0450-5036); Email: [steventaylorphd@yahoo.com](mailto:steventaylorphd@yahoo.com)

### Authors

Asitha Abeywardane – Boehringer Ingelheim Pharmaceuticals Inc., Ridgefield, Connecticut 06877-0368, United States  
Shuang Liang – Boehringer Ingelheim Pharmaceuticals Inc., Ridgefield, Connecticut 06877-0368, United States  
Zhaoming Xiong – Boehringer Ingelheim Pharmaceuticals Inc., Ridgefield, Connecticut 06877-0368, United States  
John R. Proudfoot – Boehringer Ingelheim Pharmaceuticals Inc., Ridgefield, Connecticut 06877-0368, United States  
Bennett Sandy Farmer – Boehringer Ingelheim Pharmaceuticals Inc., Ridgefield, Connecticut 06877-0368, United States  
Donghong A. Gao – Boehringer Ingelheim Pharmaceuticals Inc., Ridgefield, Connecticut 06877-0368, United States  
Alexander Heim-Riether – Boehringer Ingelheim Pharmaceuticals Inc., Ridgefield, Connecticut 06877-0368, United States  
Lana Louise Smith-Keenan – Boehringer Ingelheim Pharmaceuticals Inc., Ridgefield, Connecticut 06877-0368, United States  
Ingo Muegge – Boehringer Ingelheim Pharmaceuticals Inc., Ridgefield, Connecticut 06877-0368, United States; Present Address: (I.M.) Alkermes Inc., 852 Winter Street, Waltham, Massachusetts, MA 02451, United States. Email: [ingo.muegge@alkermes.com](mailto:ingo.muegge@alkermes.com)  
Yang Yu – Boehringer Ingelheim Pharmaceuticals Inc., Ridgefield, Connecticut 06877-0368, United States  
Qiang Zhang – Boehringer Ingelheim Pharmaceuticals Inc., Ridgefield, Connecticut 06877-0368, United States  
Donald Souza – Boehringer Ingelheim Pharmaceuticals Inc., Ridgefield, Connecticut 06877-0368, United States  
Mark Panzenbeck – Boehringer Ingelheim Pharmaceuticals Inc., Ridgefield, Connecticut 06877-0368, United States  
Daniel Goldberg – Boehringer Ingelheim Pharmaceuticals Inc., Ridgefield, Connecticut 06877-0368, United States  
Melissa Hill-Drzewi – Boehringer Ingelheim Pharmaceuticals Inc., Ridgefield, Connecticut 06877-0368, United States  
Mariana Margarit – Boehringer Ingelheim Pharmaceuticals Inc., Ridgefield, Connecticut 06877-0368, United States  
Brandon Collins – Boehringer Ingelheim Pharmaceuticals Inc., Ridgefield, Connecticut 06877-0368, United States  
John Xiang Li – Boehringer Ingelheim Pharmaceuticals Inc., Ridgefield, Connecticut 06877-0368, United States

Ljiljana Zuvela-Jelaska – Boehringer Ingelheim Pharmaceuticals Inc., Ridgefield, Connecticut 06877-0368, United States

Jun Li – Boehringer Ingelheim Pharmaceuticals Inc., Ridgefield, Connecticut 06877-0368, United States

Neil A. Farrow – Boehringer Ingelheim Pharmaceuticals Inc., Ridgefield, Connecticut 06877-0368, United States; Present Address: (N.F.) Molecular Discovery Epizyme, Inc. 400 Technology Square 4th Floor Cambridge, MA 02139, United States. Tel: 617-300-0275. Cell: 203-240-4284. Email: [nfarrow@epizyme.com](mailto:nfarrow@epizyme.com)

Complete contact information is available at:

<https://pubs.acs.org/10.1021/acsomega.1c01320>

## Notes

The authors declare no competing financial interest.

## REFERENCES

- (1) Tanaka, Y. Rheumatoid Arthritis. *Inflamm. Regen.* **2020**, *40*, 20–28.
- (2) Park, J.; Mendy, A.; Vieira, E. R. Various Types of Arthritis in the United States: Prevalence and Age-Related Trends From 1999 to 2014. *Am. J. Public Health* **2018**, *256*–258.
- (3) Scott, D. L.; Wolfe, F.; Huizinga, T. W. J. Rheumatoid Arthritis. *Lancet* **2010**, *376*, 1094–1108.
- (4) You, H.; Xu, D.; Zhao, J.; Li, J.; Wang, Q.; Tian, X.; Li, M.; Zeng, X. JAK Inhibitors: Prospects in Connective Tissue Diseases. *Clin. Rev. Allergy Immunol.* **2020**, *59*, 334–351.
- (5) Bullock, J.; Rizvi, S. A. A.; Saleh, A. M.; Ahmed, S. S.; Do, D. P.; Ansari, R. A.; Ahmed, J. Rheumatoid Arthritis: A Brief Overview of the Treatment. *Med. Princ. Pract.* **2019**, *27*, S01–S07.
- (6) Rose, B. J.; Kooyman, D. L. A Tale of Two Joints: The Role of Matrix Metalloproteinases in Cartilage Biology. *Dis. Markers* **2016**, *2016*, 1–7.
- (7) Cerofolini, L.; Fragai, M.; Luchinat, C. Mechanism and Inhibition of Matrix Metalloproteinases. *Curr. Med. Chem.* **2019**, *26*, 2609–2633.
- Jünger, A.; Ospelt, C.; Lesch, M.; Thiel, M.; Sunyer, T.; Schorr, O.; Michel, B. A.; Gay, R. E.; Kolling, C.; Flory, C.; Gay, S.; Neidhart, M. Effect of the oral application of a highly selective MMP-13 inhibitor in three different animal models of rheumatoid arthritis. *Ann. Rheum. Diseases* **2010**, *69*, 898–902.
- (8) Murphy, G.; Knäuper, V.; Atkinson, S.; Butler, G.; English, W.; Hutton, M.; Stracke, J.; Clark, I. Matrix metalloproteinases in arthritic disease. *Arthritis Res.* **2002**, *4*, S39–S49.
- (9) (a) Stickens, D.; Behonick, D. J.; Ortega, N.; Heyer, B.; Hartenstein, B.; Yu, Y.; Fosang, A. J.; Schorpp-Kistner, M.; Angel, P.; Werb, Z. Altered endochondral bone development in matrix metalloproteinase 13-deficient mice. *Development* **2004**, *131*, 5883–5895. (b) Kennedy, A. M.; Inada, M.; Krane, S. M.; Christie, P. T.; Harding, B.; Lopez-Otin, C.; Sanchez, L. M.; Pannett, A. J.; Dearlove, A.; Hartley, C.; Byrne, M. H.; Reed, A. A. C.; Nesbit, M. A.; Whyte, M. P.; Thakker, R. V. MMP13 mutation causes spondyloepimetaphyseal dysplasia, Missouri type (SEMD(MO)). *J. Clin. Invest.* **2005**, *115*, 2832–2842. (c) Engel, C. K.; Bernard, P.; Schimanski, S.; Reinhard, K.; Habermann, J.; Otmar, K.; Volkhard, S.; Weithmann, K. U.; Ulrich, W. Structural Basis for Highly Selective Inhibition of MMP-13. *Chem. Biol.* **2005**, *12*, 181–189.
- (10) Singh, A.; Rajasekaran, N.; Hartenstein, B.; Hartenstein, B.; Szabowski, S.; Gajda, M.; Angel, P.; Brauer, R.; Illges, H. Collagenase-3 (MMP-13) deficiency protects C57BL/6 mice from antibody-induced arthritis. *Arthritis Res. Ther.* **2013**, *15*, R222.
- (11) Taylor, S. J.; Abeywardane, A.; Liang, S.; Muegge, I.; Padyana, A. K.; Xiong, Z.; Hill-Drzewi, M.; Farmer, B.; Li, X.; Collins, B.; Li, J. X.; Heim-Riether, A.; Proudfoot, J.; Zhang, Q.; Goldberg, D.; Zuvela-Jelaska, L.; Zaher, H.; Li, J.; Farrow, N. A. Fragment-based Discovery of Indole Inhibitors of Matrix metalloproteinase-13. *J. Med. Chem.* **2011**, *8*, 8174–8187. Gimeno, A.; Beltrán-Debón, R.; Mulero, M.; Pujadas, G.; SGarcia-Vallvé, S. Understanding the variability of the S1' pocket to improve matrix metalloproteinase inhibitor selectivity profiles. *Drug Discovery Today* **2020**, *25*, 38–57. Amin, S. A.; Adhikari, N.; Jha, T. Is dual inhibition of metalloenzymes HDAC-8 and MMP-2 a potential pharmacological target to combat hematological malignancies? *Pharmacol. Res.* **2017**, *122*, 8–19.
- (12) Johnson, A. R.; Pavlovsky, A. G.; Ortwine, D. F.; Prior, F.; Man, C.-F.; Bornemeier, D. A.; Banotai, C. A.; Mueller, W. T.; McConnell, P.; Yan; Chunhong, Y.; Baragi, V.; Lesch, C.; Roark, W. H.; Wilson, M.; Datta, K.; Guzman, R.; Han, H.-K.; Dyer, R. D. Discovery and Characterization of a Novel Inhibitor of Matrix Metalloproteinase-13 That Reduces Cartilage Damage in Vivo Without Joint Fibroplasia Side Effects. *J. Biol. Chem.* **2007**, *281*, 27781–27791.
- (13) Maurer, T. S.; Smith, D.; Beaumont, K.; Di, L. Dose Predictions for Drug Design. *J. Med. Chem.* **2020**, *63*, 6423–6435.
- (14) Brown, A. N.; McSharry, J. J.; Adams, J. R.; Kulawy, R.; Barnard, R. J. O.; Newhard, W.; Hazuda, D. J.; Louie, A.; Drusano, G. L. Pharmacodynamic Analysis of a Serine Protease Inhibitor, MK-4519, against Hepatitis C Virus Using a Novel In Vitro Pharmacodynamic System. *Antimicrob. Agents Chemother.* **2012**, *56*, 1170–1181.
- (15) Heim-Riether, A.; Taylor, S. J.; Liang, S.; Gao, D. A.; Xiong, Z.; August, E. M.; Collins, B. K.; Farmer, B. Y.; Haverty, K.; Hill-Drzewi, M.; Junker, H.-D.; Margarit, A. M.; Moss, N.; Neumann, T.; Proudfoot, J. R.; Keenan, L. S.; Sekul, R.; Zhang, Q.; Farrow, N. A. Improving potency and selectivity of a new class of non-Zn-chelating MMP-13 inhibitors. *Bioorg. Med. Chem. Lett.* **2009**, *19*, 5321–5324.
- (16) Gao, D. A.; Xiong, Z.; Heim-Riether, A.; Amodeo, L.; August, E. M.; Cao, X.; Ciccarelli, L.; Collins, B. K.; Harrington, K.; Haverty, K.; Hill-Drzewi, M.; Li, X.; Liang, S.; Margarit, S. M.; Moss, N.; Nagaraja, N.; Proudfoot, J.; Roman, R.; Schlyer, S.; Keenan, L. S.; Taylor, S. J.; Wellenzohn, B.; Wiedenmayer, D.; Li, J.; Farrow, N. A. SAR studies of non-zinc-chelating MMP-13 inhibitors: Improving selectivity and metabolic stability. *Bioorg. Med. Chem. Lett.* **2010**, *20*, 5039–5043.
- (17) Taylor, S. J.; Padyana, A. K.; Abeywardane, A.; Liang, S.; Hao, M.-H.; De Lombaert, S.; Proudfoot, J.; Farmer, B. S.; Li, X.; Collins, B.; Martin, L.; Albaugh, D. R.; Hill-Drzewi, M.; Pullen, S. S.; Takahashi, H. J. Discovery of Potent, Selective Chymase Inhibitors via Fragment Linking Strategies. *J. Med. Chem.* **2013**, *56*, 4465–4481.
- (18) PDB accession code: SBPA.
- (19) Peters, S. A.; Petersson, C.; Blukat, A.; Halle, J.-P.; Dolgos, H. Prediction of active human dose: learnings from 20 years of Merck KGaA experience, illustrated by case studies. *Drug Discovery Today* **2020**, *25*, 909–919.
- (20) Freire, E. Do Enthalpy and Entropy Distinguish First in Class from Best in Class? *Drug Discovery Today* **2008**, *13*, 869–874.
- (21) Caplazi, P.; Baca, M.; Barck, K.; Carano, R. A. D.; DeVoss, J.; Lee, W. P.; Bolon, B.; Diehl, L. Mouse Models of Rheumatoid Arthritis. *Vet. Pathol.* **2015**, *52*, 819–826.
- (22) Skonberg, C.; Olsen, J.; Madsen, K. G.; Hansen, S. H.; Grillo, M. P. Metabolic activation of carboxylic acids. *Expert Opin. Drug Metab. Toxicol.* **2008**, *4*, 425–438.
- (23) Kashyap, A.; Singh, P. K.; Silakari, O. Counting on Fragment Based Drug Design Approach for Drug Discovery. *Curr. Top. Med. Chem.* **2018**, *18*, 2284–2293.
- (24) Barvian, N. C. et al. World Intellectual Property Organization, WO2002064568 A1 2002-08-22
- (25) Gaudilliere, B. et al. World Intellectual Property Organization, WO2003033478 A1 2003-04-24